

**DESIGN AND CONTROL OF A TELEOPERATION SYSTEM FOR
HUMANOID WALKING**

SIM WAI YONG

(B.Eng(Hons.), The University of Adelaide.)

A DISSERTATION SUBMITTED FOR
THE DEGREE OF MASTER OF ENGINEERING
DEPARTMENT OF MECHANICAL ENGINEERING
NATIONAL UNIVERSITY OF SINGAPORE

2005

Acknowledgements

First of all, I would like to thank my parents. I would not be able to complete this journey without them by my side.

I also like to thank my supervisors, Dr. Chew Chee Meng and Dr. Hong Geok Soon, for their advice and guidance during my stay in the legged locomotion group. What I have learned from them during these two years not only limited to academic and technical aspects, but also helps me to be a better grown-up.

Special thanks to my labmates - Zhouwei, Sateesh, Fengkai, Samuel and Kuang Chin. Not only for their support and valuable opinions, but also for their wonderful laughs and crazy ideas.

Thanks to all the staff members of the Control and Mechatronics Lab - Ms Ooi, Ms Shin, Ms Hamida, Mr Zhang, and Mr Yee. I could not have asked for more, they are simply amazing.

Table of contents

Acknowledgements	ii
Summary	v
1 Introduction	1
1.1 Organisation of Thesis	4
2 Background and Relevant Work	6
2.1 Bipedal Walking Control	6
2.2 Teleoperation Overview	10
2.2.1 Categories of Teleoperation System	10
2.2.1.1 Teleoperation with Mechanical Transmission	11
2.2.1.2 Teleoperation with Electrical Transmission	12
2.2.1.3 Computerized Teleoperation	12
2.2.2 Motion Control Methods	13
2.2.2.1 Joint Space Control	13
2.2.2.2 Cartesian Space Control	14
2.2.2.3 Supervisory and Traded Control	14
2.3 Applications of Teleoperation on Humanoid Walking	15
3 Hardware Configuration of the Teleoperation System	17
3.1 Overview	17
3.2 Design of the Master Exoskeleton	19
3.2.1 Design Concept	19
3.2.2 First Prototype of Master Exoskeleton	21
3.2.2.1 Components of Exoskeleton	22
3.3 PC and Decoder Unit	27
3.4 Slave (Fujitsu Humanoid Robot HOAP-1)	29
3.5 Optional Components	29
3.5.1 Head Mounted Display	29
3.5.2 LED Indicator and Audio Speaker	31
4 Kinematic Study	32
4.1 Static Anthropomorphic Measurement	32
4.2 Joint Range	33

5	Control Methods and Dimensional Parameter Study	35
5.1	Direct Mapping of Joints	35
5.2	Mapping of Foot Positions	36
5.2.1	Forward Kinematics and Jacobian	37
5.2.2	Inverse Kinematics Transformation	40
5.3	Dimensional Parameter Study	41
6	Simulation	44
6.1	Mechanical Model and Control Method	44
6.2	Joint Trajectory Acquisition	46
6.3	Ankle Joint Data Modification	47
6.4	Final Joint Trajectories	47
6.5	Model of the Ground	50
6.6	Results of Geometric Scaling	50
6.6.1	Continuous Walking	50
6.6.2	Landing Impact	52
6.7	Result of Froude Number Scaling	52
6.7.1	Body Pitch	53
6.7.2	Zero Moment Point	55
6.7.3	Gait Phases	56
6.8	Discussion of Simulation Results	57
7	Experimental Results	60
7.1	Experiment 1 - Stepping	60
7.2	Experiment 2 - Direct Mapping of Joints	64
7.3	Experiment 3 - Mapping of the Foot Position	66
7.4	Experiment 4 - Modification of Playback Time Interval	71
7.5	Experiment 5 - Modification of Walking Profile	73
8	Conclusion and Future Works	78
	References	81
	Appendices	83
A	Mass Property of Fujitsu Humanoid Robot	84

Summary

This thesis presents the design and control of a teleoperation system for humanoid. The focus of this project is the teleoperation of the sagittal plane walking. The teleoperation system consists of three major components - the master exoskeleton, PC and the slave humanoid robot.

The motivation behind this research project is to explore the possibility of the novel control method of teleoperation for humanoid walking. Two of the major factors that limit the application of humanoid robot in uncontrolled working environment are the lack of robustness in the current walking methods and lack of breakthrough in artificial intelligence. Participation of human in the control loop is appealing as this takes away the dependence of artificial intelligence.

The thesis describes the details of the mechanical design of the master exoskeleton, the control architecture of the overall system, and the control methods. Simulation result of direct mapping of human walking profile on humanoid robot is presented. Experimental results that verify the hardware system and different control method are also presented.

List of Figures

2.1	A typical teleoperation configuration	11
3.1	Overall hardware configuration of the proposed teleoperation system. Major components in the master environment include master exoskeleton and PC and decoder unit; optional components are the Head Mounted Display (HMD), LED indicator and speaker. Fujitsu humanoid robot HOAP-1 is chosen to be the slave robot.	18
3.2	Hardware setup of the proposed teleoperation system.	19
3.3	Left: Joint coordinates for the exoskeleton. Right: Human operator with the exoskeleton.	23
3.4	Top: Important part names for waist unit. Bottom: Illustration of movable parts of waist unit, along with degree of freedom and coordinates of waist unit.	24
3.5	Top: Parts breakdown drawing for thigh/shank unit. Bottom: Illustration of the degree of freedom and coordinates of thigh/shank unit. Note the jig which can be inserted into the alignment slot for the purpose of initialization of the encoders.	26
3.6	Attachment points of the master exoskeleton.	27
3.7	Schematic of the electronic circuit of the decoder unit.	28
3.8	Decoder circuit.	28
3.9	Top: Fujitsu HOAP-1 Humanoid Robot. Bottom: Joint coordinates of HOAP-1.	30
5.1	Control block diagram of the method direct mapping of joints	37
5.2	Control block diagram of the method mapping of foot positions	38
5.3	Frame attachment diagram for master exoskeleton. Left: Stance leg. Right: Swing leg.	38
6.1	Mechanical model of Fujitsu humanoid robot HOAP-1. Left: Subscript h , k and a represent hip, knee and ankle respectively, while R and L represents right and left. Right: Body pitch angle.	45
6.2	Man walking at normal speed. Muybridge (1955)	46
6.3	Top: Illustration of robot foot interfere with ground while playback the trajectory directly. Bottom: Comparison between human foot and robot foot. The ankle is the center of rotation.	48
6.4	Top: Joint trajectories for left foot. Bottom: Joint trajectories for right foot. Blue, yellow and magenta represents hip, knee and ankle respectively.)	49
6.5	Snapshots for one gait cycle. Time interval is 0.083sec.	51

6.6	Ground reaction force of swing foot after landing. Blue and red represents data for heel and toe respectively.	53
6.7	Comparison of the body pitch profile between kinematic scaling method and Froude number scaling method. The plot depicts the body pitch in one gait cycle.	54
6.8	ZMP profile of right foot during right stance phase of the gait cycle. This profile is plotted against the time of right stance phase. The y-axis value of 0 represents ZMP is located at the heel, whereas 0.098 represents toe.	55
6.9	ZMP profile of left foot during left stance phase of the gait cycle. This profile is plotted against the time of left stance phase. The y-axis value of 0 represents ZMP is located at the heel, whereas 0.098 represents toe.	56
6.10	Phase comparison between normal, foot regulated, and scaled simulations.	57
7.1	Snapshots of the stepping experiment. Snapshots are taken in the time interval of 1 second. (From left to right, top row to bottom row)	61
7.2	Right leg joint trajectories. Blue: Hip; Magenta: Knee; Yellow: Ankle.	62
7.3	Left leg joint trajectories. Blue: Hip; Magenta: Knee; Yellow: Ankle.	63
7.4	ZMP history for the stepping experiment. The red dash lines are the limit for the ZMP value, which is maximum +43 and minimum -26. ZMP for right and left foot are represented in yellow and turquoise lines respectively. The boxes at the bottom of the graph are the state of the humanoid robot - bright green: right foot lifted; light green: left foot lifted; yellow: double support.	63
7.5	Walking sequence of direct teleoperation. The humanoid robot shown instability during landing of swing foot and eventually fall at the second step.	65
7.6	Illustration of the difference in timing for the landing of the swing foot. Arrow-a: Human operator has landed his swing foot. Arrow b: Left leg of the humanoid robot is yet to land.	65
7.7	Walking sequence of teleoperation by mapping of the foot position.	67
7.8	Walking sequence of the humanoid. Notice the first snapshot, the knee of the humanoid robot is bent even human operator is stand with straighten knee. This is a measure to prevent singularities in the Inverse Kinematic algorithm.	68
7.9	Comparison of the knee configuration of Direct joint mapping method and Foot mapping method.	68
7.10	Leg joint trajectories for experiment 3.	69
7.11	Foot trajectories for experiment 3.	70
7.12	Snapshots of the experiment of scaling based on modification of playback time interval.	72
7.13	Snapshots of the experiment of scaling based on modification of walking profiles. Notice the small stride length and step height of the robot.	74
7.14	Leg joint trajectories for experiment 5. Blue: Hip; Magenta: Knee; Yellow: Ankle. Notice the scaling down of the joint angles of the slave compare with the master.	75
7.15	Foot trajectories for experiment 5. Blue: Vertical foot position; Yellow: Horizontal foot position. Notice the scaling down of the foot position of the slave compare with the master.	76

List of Tables

3.1	Specification of US-Digital E3 Encoder	21
4.1	Link length comparison between human and Fujitsu humanoid robot . .	34
4.2	Joint range comparison between human and Fujitsu humanoid robot . .	34
6.1	Comparison of body pitch profile between geometric scaling method and Froude number scaling	54
A.1	Mass Property of Fujitsu Humanoid Robot	85

Chapter 1

Introduction

Robot holds the advantage of being less susceptible to hazardous working environment over human. As wheeled robot has less maneuverability in rough terrain and unstructured environment, it is foreseeable that legged robot, especially, the humanoid robot will be an important workforce in harsh and extreme working conditions, for example, the presence of intense heat and smoke in fire disaster area, or radiation in the nuclear plant, etc. Taking advantage of the advancement in bipedal walking control, several humanoid robots, namely the Honda Asimo (Hirai, 1998) and Sony Qrio (Kuroki, 2003), have recently showcased the capability of walking not only on flat surface, but also on terrain of limited unevenness. However, their adaptability to natural environment is somehow still rather limited.

The use of a fully autonomous humanoid robot, which should not only be able to complete the task given, but also perceived and react in accordance to the unstructured environment, is unlikely to be realized in the near future. For a robot to be able to function independently and complete the tasks in a highly varied environment, the crucial element is a well developed and competent artificial intelligence. Unfortunately, the research and development of artificial intelligence is yet to keep pace with the progress of hardware technology.

A typical example to illustrate the complexities and difficulties of utilizing a autonomous robot in real environment is the task of approach, identify and capture. The

scenario can be very simple, at least for humans - to walk across an office layout with cubicles and pick up a cup from the table. To accomplish the task, the robot has to know where it is at, where the destination is, which path to take, which cup to take, and how to take it. The process for these tasks can be divided into two categories - low level process and high level process.

Low level processes include localization, image processing, sensor data acquisition and fusion, and local control of the actuators. The task of localization and image processing is somewhat related closely, as the former rely on the output of latter. Localization involve two basic subtasks - mapping of the surroundings and depth map generation. Image processing is vital such that information about the surroundings and robot itself is acquired accurately. Hence an advanced and effective image processing algorithm is required, such that the effect of variables, such as lighting conditions, can be minimized. In contrast to the state of sensor technology, the process of sensor data fusion is still elementary. Sensor data fusion is the combination of redundant sensor information into a useful and accurate one. It is obvious that to be able to process the above three tasks, high computing power is required onboard for autonomous robot. The control of the actuators is the least problematic task of the four. High accuracy tracking of the trajectory of DC motors, the most commonly used actuator in robot, is achievable nowadays thanks to the advanced and continuous research of the controller.

High level process involve strategic and decision making. One of typical tasks is the process of path generation - how to get to the destination. Path generation is an online process. Basically, the robot needs to know which way to go and how to get there. This usually consists of choosing different motion patterns according to situations, which require a huge bank of motion patterns. Obviously a powerful artificial intelligence is needed in order to deal with the entire unknown situations in the unstructured environment. Such a well-developed artificial intelligence is not yet available at the moment, and it is difficult to say when this area will have a break through such that artificial intelligence can be at least comparable to an infant.

From the example elaborated above, it is expected that a partial autonomy in the robot system would be a solution that will overcome the current limitation and difficulties

of robot deployment in the real working environment. The allocation of the tasks in this partial-autonomous system should take into account of the strengths, capabilities and limitations of the humans and robots. Humans in general are good at perceptions and understanding, task decomposition, problem solving and replanning of fault recovery, while robots are better at low level sensory and control functions, trajectory planning, precision motion, performing routine and repetitive tasks. By combining the strengths of two parties, the replacement of robots in the hazardous working environment can be realized soon.

The participation of human in the control loop of a robot system is not a new idea, however most of the research is done on robot manipulators with a fixed base. The application of teleoperation on humanoid walking is relatively rare; consider only two cases so far in the world - Honda robot (Hirai, 1998) and HRP-1S (Kaneko, 2002). Nevertheless, due to the supervisory control nature (Hannaford, 2000) of the teleoperation system applied on those two cases, the robots are still not able to adapt to the highly unstructured environment. Some of the limitations include the following:

1. Landmarks for environments are needed for visual processing.
2. Staircase parameters such as height, width and numbers of steps need to be known.
3. Relatively complex system as the supervisory control involve only high level commands, low level processing such as visual processing, motion generation are still a burden of the robot.
4. A huge motion data bank is needed to adapt to the unstructured environment.

A novel approach to extend the walking capability of humanoid robot by means of teleoperation (Sim et al., 2004) has been introduced. The novelty of the proposed system is the difference of the control method with other research works. Instead of passing the high level command to the robot through the computer console and let the humanoid to generate walking motion itself, the proposed system actually make the control of the humanoid walking more intuitive. By wearing the exoskeleton type master interface, the leg motion of the human operator can be either directly map to the humanoid, or

the human can control the foot placement of the humanoid during locomotion. This way, the human operator is able to control the humanoid as if he himself is the robot, and at the same time the humanoid robot has the advantage of better adaptability to unstructured environment.

This thesis describes the details of the design and control of the teleoperation system for humanoid walking. The design process of the master exoskeleton, the control architecture and the electronics implementations are discussed. Dimensional analysis is also included in this thesis to investigate the applicability of different scaling methods. The simulation result and experimental result are also presented in this thesis.

1.1 Organisation of Thesis

The thesis proceeds as follows:

Chapter 2 gives the background study for this thesis. Various control approaches for humanoid walking and their limitations are discussed, followed by an overview of teleoperation and its application.

Chapter 3 presents the hardware configuration of the teleoperation system. Design of the master exoskeleton will be discussed in detail. The selection of encoders, technical specifications of the design and the design strategy are explained.

Chapter 4 presents the kinematic study of human and humanoid robot. A comparison between human and humanoid robot will be discussed. Feasibility of the proposed teleoperation system will be proven.

Chapter 5 introduces the control method of the teleoperation system. Dimensional analysis will also be included in this chapter.

Chapter 6 gives the details of the simulation result of the two scaling methods. This chapter will include the details of the simulation approaches and analysis of the result.

Chapter 7 presents the experimental results of the teleoperation system. Five experiments has been conducted to test the system, namely the hardware evaluation test, experiment of direct mapping of joints, experiment of mapping foot positions, and ex-

periment on two different scaling methods.

Chapter 9 concludes the thesis with a discussion and advice on future research.

Chapter 2

Background and Relevant Work

In this chapter, some background and relevant work will be presented. Section 2.1 presents the various control methods that researchers adopt for bipedal walking. Section 2.2 is an overview of teleoperation and classifications of the control methods of teleoperation system.

2.1 Bipedal Walking Control

Achieve stable walking for humanoid robot is a difficult task. Some of the major issues associated with control of bipedal locomotion are listed as followed (Vukobratovic, 2004):-

1. Bipedal systems are high-order highly-coupled nonlinear dynamical systems.
2. The discrete changes in the dynamic phenomena. The locomotion mechanism changes from open to a closed kinematic chain during a single walking cycle.
3. The underactuated degree of freedom between the support foot sole and the ground cannot be controlled directly.
4. The uncertainty of the walking surface and environment.
5. The capability of the mechanical implementation due to the limitation of the actuators, which included consideration of the size, power to weight ratio etc.

From the point of view of the center of gravity, bipedal locomotion can be divided into two categories - static walking and dynamic walking. In static walking, the projection of the center of gravity on the ground is always kept within the support foot area. As this kind of locomotion is named - the dynamic effect is negligible, which means that the humanoid robot has to move in a relatively slow motion. Another characteristic of such kind of locomotion is that at anytime the humanoid robot stop its motion, it will remain in the stable position indefinitely.

Dynamic walking is much complicated in terms of control, maintenance of balance and also the generation of a valid walking pattern. Nevertheless, dynamic walking is a better approach due to the fact that dynamic walking provides faster walking speed and greater efficiency than static walking. For this reason, studies on dynamic walking has been the focus of researchers worldwide. The walking control method can be classified into five groups - model based, ZMP (Zero Moment Point) based, biological inspired, learning, and divide-and-conquer.

Model-Based Method The principle of model-based method of biped walking control is straight-forward - by applying law of physics, a mathematical model of the biped robot is derived and to be utilized in the synthesis of control algorithm. The most notable example of this category is the Linear Inverted Pendulum model proposed by S. Kajita (Kajitha et al., 1991). It is considered the simplest model that describe the bipedal locomotion. The model of Linear Inverted Pendulum describe the motion of the center of mass (COM) of a planar biped with mass-less legs. During single support of the walking cycle, the motion of the COM behaves like a point mass inverted pendulum with variable length. The dynamic equations of the linear motion of the COM can be solved analytically. The trajectory of the joints of the biped robot can be found by using inverse kinematics and tracked by simple position control. Ankle torque is used to compensate for any disturbance or errors in the model. This simple control method has been realized in the real robot Meltran.

Advantage of this method is its simplicity and the analytical closed-form solution. However, this method is limited to situation which the ground profile is known and well-

defined, as the constraint line of motion of the COM of the model is defined with respect to the ground. Another pitfall of this method is the consideration of the dynamic effect of the swing leg as a disturbance, which is compensated by the ankle torque. As the ankle torque of the biped robot is limited due to underactuation nature of the support foot sole and the ground, the effectiveness of such disturbance-compensation would be hindered.

The Linear inverted Pendulum model has been extended to 3-D recently (Kajitha, 2002). The control method has been utilized in the robot Meltran II to prove its applicability.

ZMP Based Method The concept of Zero Moment Point (ZMP) has gained wide acceptance since it was introduced in 1973 (Vukobratovic, 1973). ZMP has been playing a crucial role in solving the biped robot stability and dynamic walking pattern synthesis. Zero Moment Point is defined as the point on the ground in which the sum of all moments of the active torques equals to zero. If the ZMP is within the convex hull of all contact points between the foot and the ground (support polygon), the robot will walk in a dynamically balance fashion.

This method can be used in two ways - walking pattern synthesis and verification of a walking pattern's stability. By means of walking pattern synthesis, researchers preplanned ZMP profile such that it is within the support polygon at all time during the walking cycle, the trajectory of COM of the biped robot is then calculated. Similar to the case of Linear Inverted Pendulum method, once the trajectory of COM of the biped robot is obtained, the trajectory of all the joints of the biped robot can be found by using inverse kinematics.

In the second approach, the ZMP criteria is served in later part of an offline joint trajectories planning as a verification of stability. The offline trajectory planning is one of the most elementary method to control a biped walking. Among them, the simplest and most intuitive way of obtaining the joint trajectories is to record the human motion and post-process the data such that it satisfy the ZMP criteria in simulation before implementing in the real robot. It is expected that this method requires much effort in

tuning as the trajectory which works in simulation might not work in real robot. This method has been used in the development stage of the Honda robot.

Biological Inspired Method Biological inspired method is based on the belief of the possibility of extracting information from biological system - living life, that can be implemented on artificial system. One of the most extensively used approaches is the Central pattern generation (CPG).

Evidences have been widely accepted as a support to the hypothesis that there exists neural networks in the spinal cord of animals (also humans), referred to as "central pattern generators" (CPGs), that are capable of producing rhythmic movements, such as swimming, walking, and hopping. Several researches have been conducted in order to extract this piece of information and implement in biped robots (Zielinska, 1996; Taga, 1995; Jalicis at al., 1997). The generation of the periodic signals - reference joint trajectories, is created by using a coupled Van der Pol nonlinear oscillator equations. If the signals are generated in an appropriate way, the biped is able to walk stably.

Learning Method Learning method has been used in systems that is complex and difficult to model. It is hardly surprising that researchers have been playing with the idea of implementing learning method on bipedal walking. Neural Networks and Reinforcement Learning are the two popular learning tools that researchers used. Successful example of implementation of Neural Networks in bipedal walking include Miller, Reil and Hu. Reinforcement learning was extensively used in the research of Chew and Pratt (Chew et al., 2002), and Benbrahim and Franklin.

Divide-and-conquer Method Divide-and-conquer method is the practice of breaking a complex problem into small and simple problems. Bipedal walking is a complex and difficult control problem. Generally speaking, 3-D bipedal walking can be divided into frontal plane, transverse plane and sagittal plane walking; or even a smaller number of subtasks. This approach has been illustrated by the research work of Raibert and Pratt.

2.2 Teleoperation Overview

”Teleoperation” technology support a form of control in which the human directly guides and causes each increment of motion of the slave (Hannaford, 2000). Typically the slave robot follows the human motion exactly. However in some more advanced and computer mediated system, there may be coordinate transformation imposed between the master and slave. A teleoperation system generally sends one of the conjugate variables (either force or velocity) from the operator side to the slave. If the conjugate variable is sent back from the slave and transferred to the operator, a virtual energetic link can be created.

In general, three environments exist for teleoperation system: master environment, slave environment and X environment (Vertut, 1985). The master environment houses the human operator and the control system. The role of the human operator can be divided into action, sensing and decision making. The control system can be anything ranging from some special mechanical structure, or even a pointing device, to a computer console. The slave environment corresponds to the work area of the slave, which is located some distance away, or separated by some physical barrier from the master environment. The X-environment, generally refer to the content of a certain task to be accomplished in the slave environment. It is situated in human operator’s mind in reality. A general configuration of teleoperation is depicted in Figure 2.1.

2.2.1 Categories of Teleoperation System

Teleoperation systems can be divided into three categories based on their functional complexity and channels of data transmission. The three categories are teleoperation with mechanical transmission, teleoperation with electrical transmission and computerized teleoperation (Vertut, 1985).

What is common in these three categories of teleoperation system is the role of the human operator. The role of the human operator can be divided into three groups internally - mechanical actions, sensing abilities and decision making abilities. The properties of these categories are described as below:-

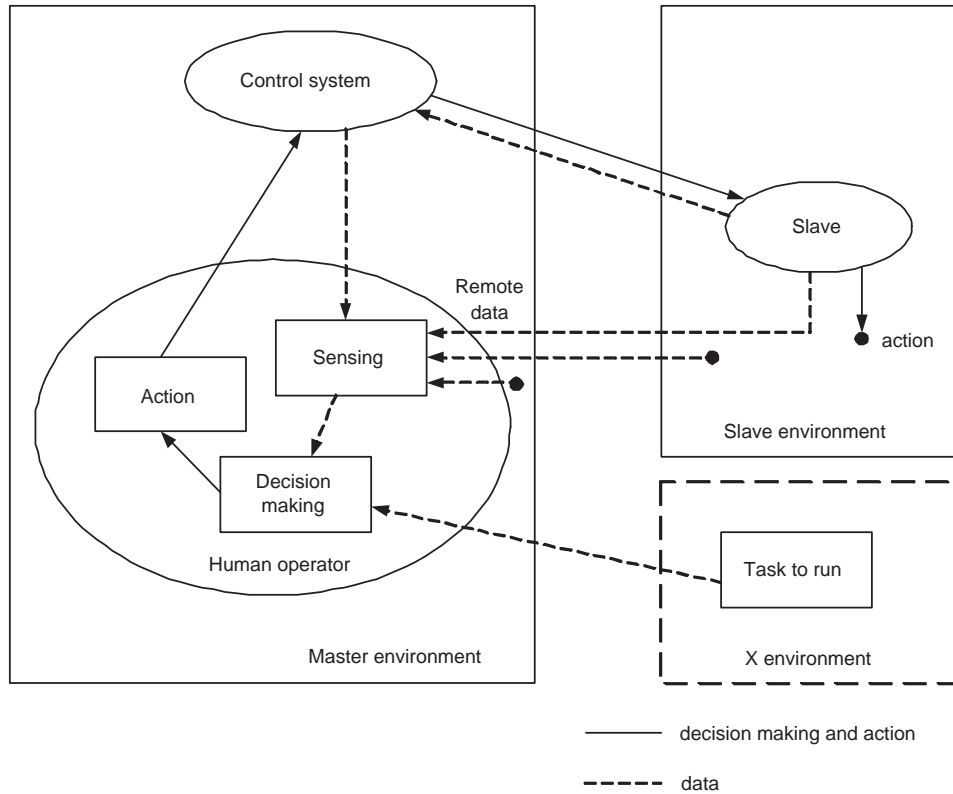


Figure 2.1: A typical teleoperation configuration

1. Sensing - receives data from the external environment (both master and slave) and transmits to the brain.
2. Decision making - based on the data from sensing operator and the knowledge of the task and make necessary decision.
3. Mechanical action - taking the command of the decision making operator and generation of physical actions to be realized in the real world.

2.2.1.1 Teleoperation with Mechanical Transmission

This is the most elementary teleoperation system. The earliest teleoperation system is realized in this mode. In this type of teleoperation system, a mechanical link is constructed between the master environment and slave environment. Usually the master and slave is separated by a shielding which allows the human operator to view the slave environment through a transparent window. This type of system involves little or none of the electronics as the movements are transmitted mechanically. Typical application

is the handling of radioactive or biohazard materials in research lab.

2.2.1.2 Teleoperation with Electrical Transmission

In this type of teleoperation system, the mechanical link between the master and the slave is replaced by an electrical link. In this mode, the distance between the master and the slave is now increased significantly. However, some undesirable side effects occur due to the increase of this physical space separation. Some of the major drawbacks include the loss of direct vision feedback, the loss of direct force feedback and the effect of time delay.

Solutions to these drawbacks have been resolved, to certain degree by some of the researchers. Partial vision feedback from the slave environment is able to restore by using cameras. Force feedback can be regenerated by artificial synthesis force based on the measurement of torques/force experienced in slave. However, performance of the teleoperation is generally reduced as these substitution is just limited replication of the the direct feedback.

2.2.1.3 Computerized Teleoperation

One way to solve the problems of teleoperation by electrical transmission is to introduce a computer in between the master and slave as a second operator. This second operator has limited capability as of human - limited ability of sensing and decision making. The second operator will, ideally, facilitate the teleoperation by assisting in the appropriate decision making and action. However this will increase the complexity of the system and required careful and complicated design.

Other than the introduction of this second operator, the more recent development of the computerized teleoperation is the introduction of virtual environment. By replicate the slave environment using computer graphics, researches shown a significant improvement of teleoperation using this kind of virtual graphic feedback.

2.2.2 Motion Control Methods

Other than the direct transmission of motion of teleoperation system with mechanical transmission, there are three types of motion control method. Joint space control basically is limited to those systems in which the kinematic similarity between master and slave is apparent. Cartesian coordinate control is usually used where the orientation of the end-effector of the slave is not critical. These two control method is used in the teleoperation system with electrical transmission. The last category of motion control method is the computerized teleoperation. Computer is added into the control loop to assist human operator.

2.2.2.1 Joint Space Control

In some teleoperation systems, the motions of the human operator must be continuously reproduced by the slave robot. Normally, the master and slave arms are kinematically (geometrically) identical within a scale constant. In this case it is adequate to transmit the angles of the individual joints of the master robot arm. Because of the kinematic similarity, the motion of the slave's end effector will exactly follow that of the master if the slave's joints follow the same trajectory as the master's joints. Both the master and slave side motion can therefore be represented in joint coordinates.

A special case of communication arises when the joint coordinates transmitted from the master side are those of the human arm itself - exoskeletons. The human operator wears an exoskeleton - actually a robotic mechanism into which the human's arm can fit, and the joints of the exoskeleton are aligned with the human joints. The slave robot must then have the same kinematic equations as the human arm. One advantage of this approach is that it is relatively easy to design an exoskeleton that can track the entire workspace of the human arm. Apart from the difficulty of wearing the exoskeleton, initialization of the system is also a problem. Initialization is critical for this type of control method as any offset during the initialization of the exoskeleton will seriously jeopardize the performance of the teleoperation.

2.2.2.2 Cartesian Space Control

Joint coordinates control might not be feasible for some application, such as when the master device have to be operated in a confined space. In this case, it is essential that the master and the slave can be kinematically different. Instead of controlling every joints of the slave, the master control only control the end-effector's cartesian position. Joystick is the most commonly used master device for this type of teleoperation. The teleoperation systems developed in which the master and slave have different kinematic designs are sometime called generalized teleoperation system.

2.2.2.3 Supervisory and Traded Control

The third kind of control method is developed for the purpose of eliminating the problems associated with joint coordinates. For telerobots, only goals are communicated, so that this requirement is relaxed. Sheridan used the term "Supervisory Control" to denote a type of control in which goals and high level commands are communicated to the slave.

Although supervisory control in principle avoids the need for a pointing interface, such as a master manipulator or exoskeleton, one is sometimes included to overcome the limited capability of the autonomous slave. Situation such as this is quite common as some skills or procedure needed of an application cannot be performed by an autonomous system at the slave site. It is expected when the environments are highly structured and external perturbations and uncertainty are kept minimal; pointing devices are not required. On the other hand, in order to have a high degree of confidence of task completion in an uncertain environment, both teleoperation and supervisory modes are needed. In practice, the control teleoperation systems are often switch between human (teleoperator) and computer (telerobot). These systems can be termed "traded control" because low level control of the slave robot motion passes back and forth between human operator and robot.

2.3 Applications of Teleoperation on Humanoid Walking

Despite the widely recognized benefits of teleoperation in uncertain environments, not many researches have been done for the teleoperation of the humanoid walking. In fact, only two notable publications are found. Both publications are from research institutes which can be considered as leaders in the humanoid research in Japan.

The first one is reported by the researchers of Humanoid Robotics Project (HRP) (Hasunuma, 2002) sponsored by the Ministry of Economy, Trade and Industry (METI) of Japan. The main purpose of the paper is to describe the results of investigations and experiments as for proxy drive of a forklift by humanoid robot HRP-1. The teleoperated humanoid robot platform consists of a humanoid robot (HRP-1), and a remote control cockpit system. The control of the bipedal walking is input directly using a display screen with the 3D mouse as a command input device. The parameters for the bipedal walking are the desired position x , y and orientation with relative to the current position and orientation; and the high level command of walking up or down a number of steps of the staircase. As this experiment is focused more on the task of teleoperated driving of forklift, it is designed relatively simple for the walking. The humanoid is only required to walk up a staircase to the driving position of the forklift. The experiment result demonstrates the idea of using teleoperation in order to extend the limited capability of humanoid in real application.

The second paper is the work by Hirai et al. (1998) for the Honda robot. The team has constructed an integrated system for the Honda robot which can automatically perform certain tasks in a known environment, and tasks in an unknown environment with the assistance from a human operator. The integrated system consists of the robot itself and its teleoperation console. The functional blocks of teleoperation console consists of the user interface, action planner, environment map and dynamics control module of the master arm. The operator inputs the basic locomotion path and action to the user interface. The action planner modifies the basic plan by the vision processing result and sends the basic action commands such as "go straight", "turn", "go up stairs", and so forth. In the environment map, there are the information of the position and the

landmarks, the shape parameters of the stairs, etc. Using these function modules, the robot is able to walk autonomously according to the locomotion path.

However, due to the supervisory control (Hannaford, 2000) nature of the teleoperation system applied on those two cases, the applications of robots are still limited to structured environment. Some of the limitations include the following:

1. Landmarks for environments are needed for visual processing.
2. Staircase parameters such as height, width and number of steps need to be known.
3. Relatively complex system as the supervisory control involves only high level commands, low level processing such as visual processing, motion generation are still a burden for the robot.
4. A huge motion bank is needed to adapt to the unstructured environment.

Chapter 3

Hardware Configuration of the Teleoperation System

3.1 Overview

By using the general mechanical teleoperation framework (Vertut, 1985), a concept of teleoperation system for humanoid robot has been constructed. The master environment consists of two major components, which are the master interface and the head mounted display. As for the slave environment, a HOAP-1 Fujitsu Humanoid is used as the slave. A PC acts as the main controller interfacing between the master and slave.

The master interface is an exoskeleton type of mechanical linkage which attached to the human operator. The function of the master interface is to capture the joint information in our teleoperation system. It is designed such that the linkage is kinematical similar to the robot leg, with each joint equipped with an incremental encoder. The major advantage of having such an interface is it makes the control of the robot leg easy - straight forward mapping the angle to the slave, and the human operator can control the robot leg intuitively.

The encoder data captured from the exoskeleton is then transfer to the PC before sending to the slave in real-time, either by using a LAN or USB cable. The visual data obtained through the robot's camera will be displayed through the head mounted display

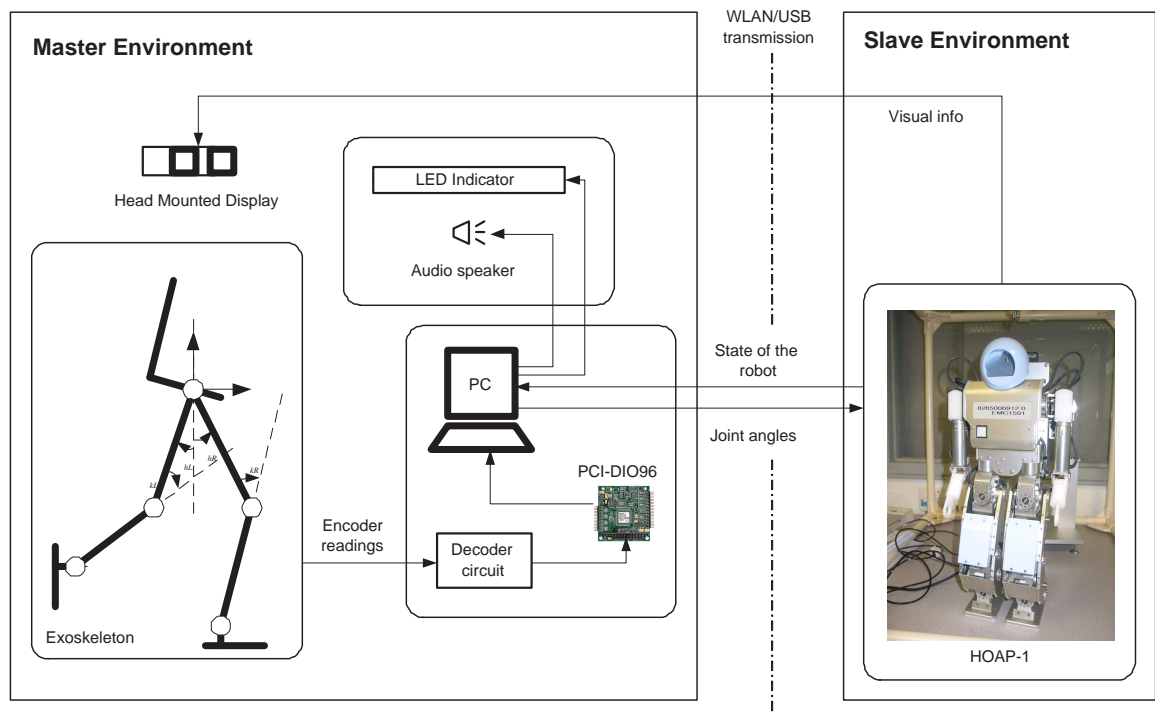


Figure 3.1: Overall hardware configuration of the proposed teleoperation system. Major components in the master environment include master exoskeleton and PC and decoder unit; optional components are the Head Mounted Display (HMD), LED indicator and speaker. Fujitsu humanoid robot HOAP-1 is chosen to be the slave robot.

such that the human operator can see what the robot sees and use the information to access the condition of the robot. This piece of hardware is for the purpose of future development of the teleoperation system. Audio speaker and the LED indicator are optional hardware which provides the indirect feedback (ZMP position) from the slave.

The slave, HOAP-1 Fujitsu Humanoid, has 6 Degree-of-freedom (DOF) for each leg. However in sagittal plane, only three pitch angles of the hip, knee and ankle are needed to be controlled. In order to investigate the true sagittal plane walking, a support frame has been constructed such that the robot will be constrained in the sagittal plane.

The overall system architecture is presented in Figure 3.1. The experiment setup is shown in Figure 3.2.

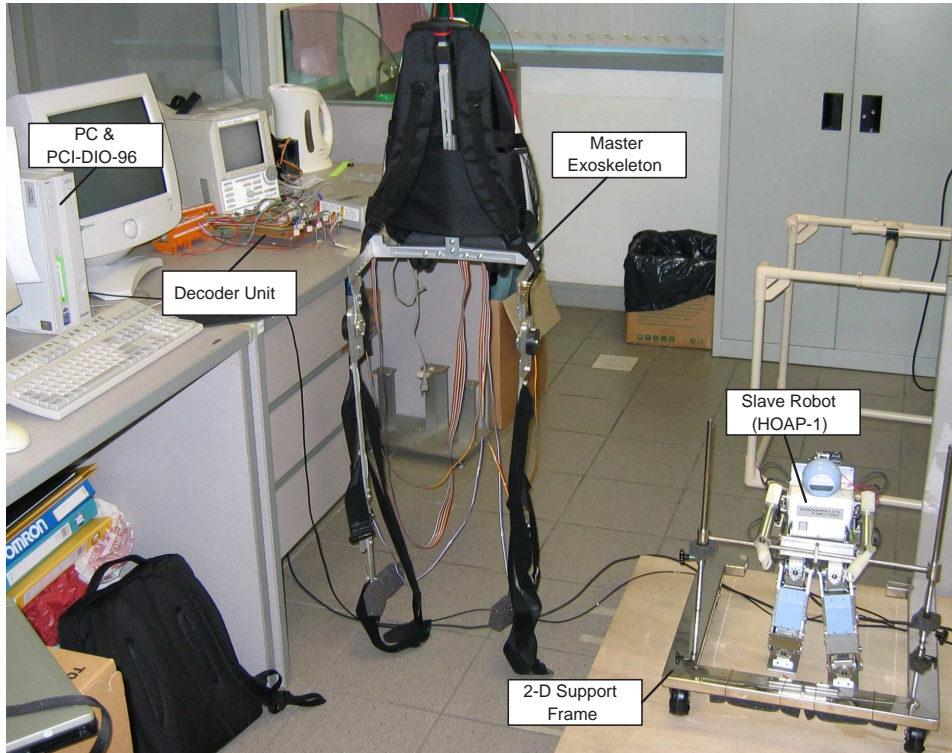


Figure 3.2: Hardware setup of the proposed teleoperation system.

3.2 Design of the Master Exoskeleton

The master interface is the most important component in any of the teleoperation system. The key feature of the proposed teleoperation system is the form of master interface, which can be worn by human operators and is kinematically similar to the slave - a master exoskeleton. The function of the master interface is to capture the joint information of the human operator in our teleoperation system. The major advantages of having such an interface are it makes the control of the robot leg easy - straight forward mapping the angle to the slave, and the human operator can control the robot leg intuitively.

3.2.1 Design Concept

The design of the master exoskeleton structure must address the fact that the structure's primary function is to capture the joint movement of the human operator and act as a control device in the system. The fundamental concept of the design is based on the

idea of tracking the human operator joint by joint, hence the design should be highly anthropomorphic. In addition, the exoskeleton is wrapped around the lower limbs of the human operator with the objective of minimizing disturbances exerted on the operator. Following these requirements in the design process has desirable effects on the actual implementation of the teleoperation system. The decision on the features of the master exoskeleton such as the number and location of the joints, the location of the attachment points, length of the linkage between joints, can be reached easily based on intuition.

Human anatomy is used as a reference for the design of the master exoskeleton. It is widely known that the human legs have redundant joints; thus, there are multiple configurations for each unique foot position or orientation. The existence of redundant joints means an increase of degree of freedom and hence increase of system complexity. A survey of the humanoid robots nowadays readily reveal the most common number of joints for lower leg are fixed to six, which is the minimum requirement to be able to achieve human-like 3-D walking.

One of the major problems of designing the master exoskeleton is the co-locating of the joints for human operator and the structure. To have both the joint of the human operator and the joint of the master exoskeleton rotate about a common axis is difficult, in particular the hip joint, which has multiple degree of freedom; and knee joint where the center of rotation is not fixed. What complicates further is the wide range of human operator size, the variation of the limbs has a direct impact on the accuracy of the co-locating of the joints. Such disparity of the axes will result not only in tracking errors, it is also possible that the structure will obstruct the motion of the human operator.

This problem can be resolved by having a complete design of structure that resemble human leg perfectly with all the redundant joints. However it is not feasible as it will be time consuming and require in-depth study of human anatomy. This problem can only be minimized by careful study and design of the master exoskeleton, such that the joints are co-located as close as possible.

Location of the attachment points plays a crucial role in the performance of the master exoskeleton. An inappropriate location of the attachment of the structure will definitely lead to a difference in the motion of the master exoskeleton and human oper-

Table 3.1: Specification of US-Digital E3 Encoder

Rate	0 - 100,000 cycles/sec
Resolution (CPR)	64 - 2048 cycles per revolution
Resolution (PPR)	256 - 8192 pulses per revolution
Voltage supply	5V

ator. The principle of design is that for each link there will be two attachments above and below respectively.

3.2.2 First Prototype of Master Exoskeleton

The function of the first prototype of the master exoskeleton is to capture the sagittal plane (2-D) walking profile of the human operator. Results from kinematic study and simulation show that the ankle of the humanoid robot should be controlled passively to overcome the difference in foot structure between humanoid robot and human. As a result, the joint information required to be captured are hip pitch and knee pitch only.

The design of the first prototype of the master exoskeleton emphasize on the anthropomorphism. As the proximity of the exoskeleton to the human joints is maximized, human operator is possible to control the robot lower limbs as his own. Notice the kinematical similarity in sagittal plane of the lower limbs of human and humanoid robot, the possibility of direct mapping from one to another is justified; therefore the control of the sagittal plane locomotion.

The rotary encoder chosen is US-Digital E3. It is an optical incremental rotary encoder. Some of the selection considerations include cost, size, response rate and resolution. As the master exoskeleton is utilized in relatively slow tracking and requires less accuracy, the US-Digital E3 is more than capable of fitting the criteria. Some of the specifications are listed in Table 3.1.

Figure 3.3(Left) is the joint coordinates for the exoskeleton, which corresponds directly to those of the humanoid robot for ease of direct mapping. Knowing that the ankle joint is redundant in sagittal plane walking on level ground, a total of four en-

coders are being fixed at the hip and knee joints of the master exoskeleton respectively. Figure 3.3(Right) shows the joints coordinates and the 1st prototype of the master exoskeleton in action. (The dashed line represented the virtual existence of the ankle on the master exoskeleton - ankle is regulated to be parallel with ground).

Some of the important features are shown as following:-

1. Anthropomorphic structure - the joints are located as close proximity as the human's.
2. Light weight - the master interface should not provide excessive load to the user, hence the choice of light weight material of aluminium.
3. Back pack provide good attachment to the human operator's body.
4. Velcro straps for firm attachment of the structure to human operator's leg.
5. Four rotary encoder in total are used to obtain the required data - hip pitch (x2) and knee pitch (x2).
6. Extra joint at the hip (hip yaw) to prevent restricted and unnatural motion.

3.2.2.1 Components of Exoskeleton

The exoskeleton can be divided into three essential units, namely the waist unit, the thigh unit and the shank unit.

Waist Unit The waist unit is the base of the master exoskeleton. It is designed as a rigid frame that is attached to a backpack with shoulder strap. The reason for choosing the backpack is that it is a ready-made solution for the problem of close and comfortable attachment of the structure to the human operator's body.

One of the most important design consideration of the master exoskeleton is the close proximity of the joints between human operators and the master exoskeleton. For waist unit, it is important that the center of rotation of the hip of both master exoskeleton and human operator should be as close as possible.

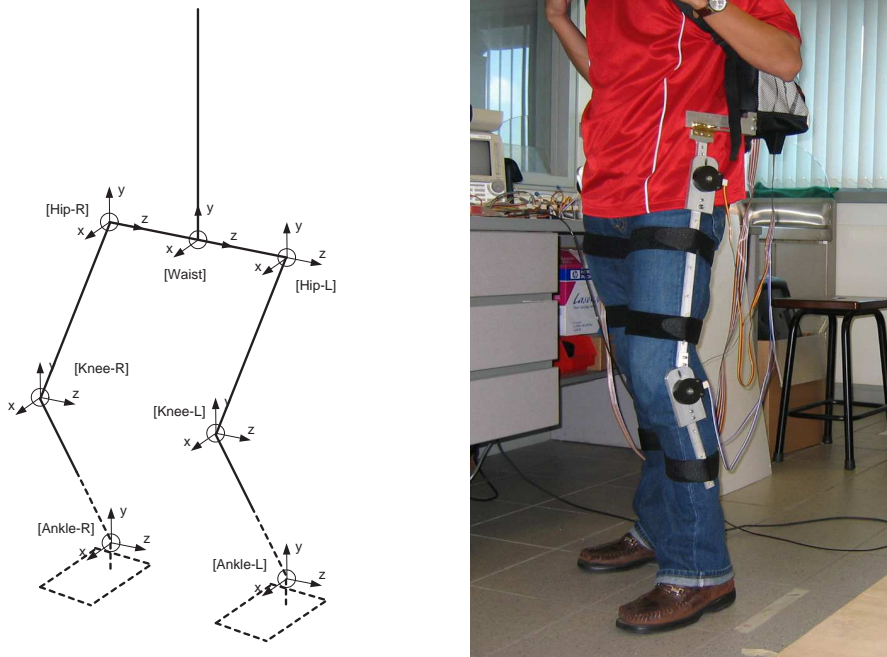


Figure 3.3: Left: Joint coordinates for the exoskeleton. Right: Human operator with the exoskeleton.

As the center of the rotation of the hip pitch of human operator can only be determined experimentally, two moveable parts - back connection plate and hip connection plate are designed to resolve this problem, as illustrated in Figure 3.4. Back connection plate is designed such that the height of the waist unit can be adjusted along the slot of the back plate. The slot on the side wings provide the possibility of horizontal adjustment of the hip connection plate. Together they provide a reasonable range of adjusting the structure such that the hip joint of the master exoskeleton is in close proximity with the human operator.

There is a hinge connection between the side wing and hip connection plate. This hinge provides a degree of freedom - hip yaw, for the structure. Even though only pitch angles of the joints are needed to control sagittal plane walking, hip yaw is included here for the comfort of the human operator. Human operator is observed to walk in an awkward and unnatural fashion if such degree of freedom is not included in the master exoskeleton.

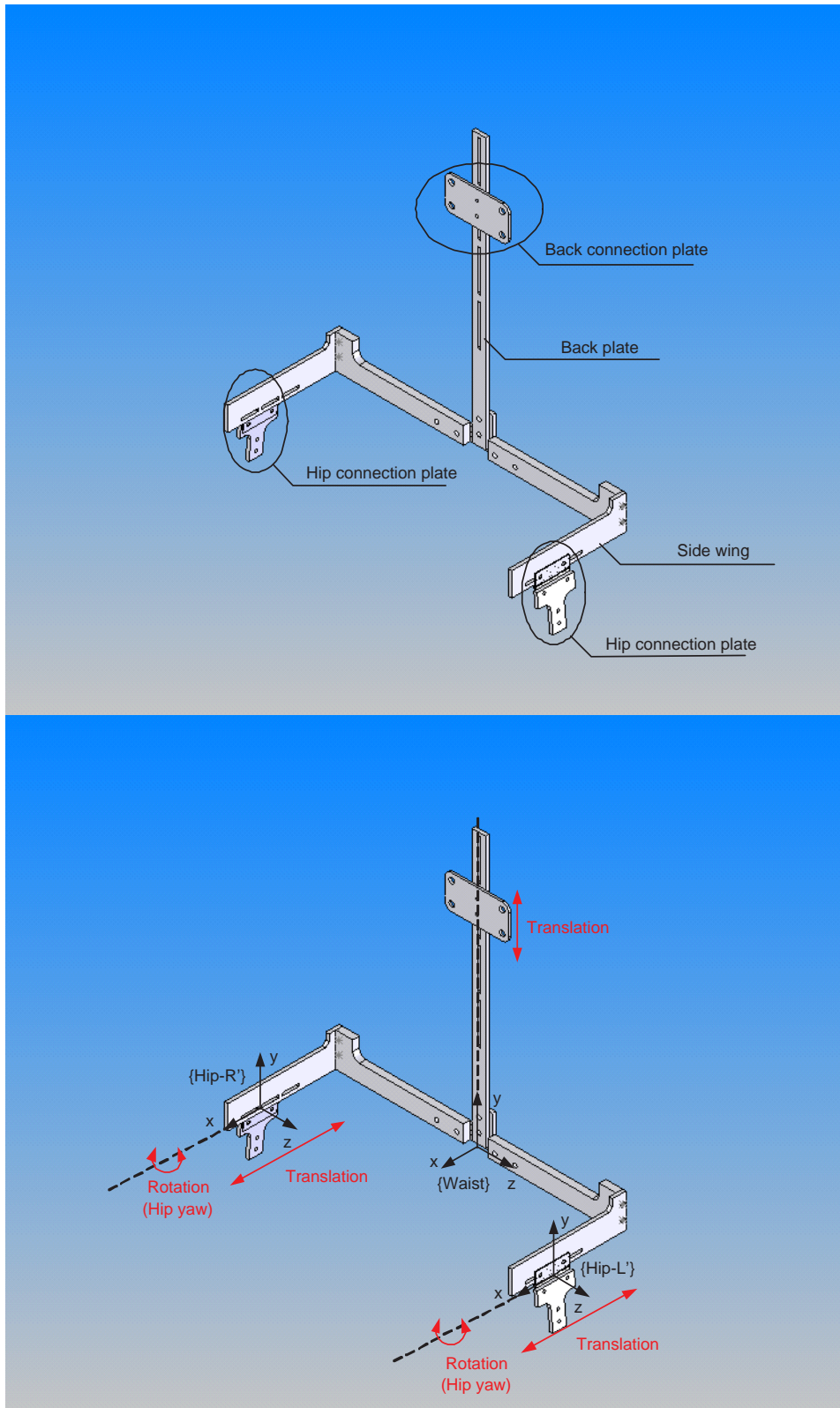


Figure 3.4: Top: Important part names for waist unit. Bottom: Illustration of movable parts of waist unit, along with degree of freedom and coordinates of waist unit.

Thigh and Shank Unit Same mechanical structure design has been adapted for the thigh and shank. One of the main reason is to reduce the number of different parts. Common parts not only reduce the complexity in fabrication, but also improve the ease of assembly. The detail design of the thigh unit is shown in Figure 3.5.

Initialization of the incremental encoder of the master exoskeleton is important as it has direct impact on the accuracy of the position tracking of the master exoskeleton. Alignment slots on link 1 and link 2 is used to solve this problem. A jig is meant to be inserted into the alignment slot in order to secure a fix position upon initialization. This alignment slot and the jig has the clearance of $\pm 0.5\text{mm}$.

Attachment Point Attachment points are important to enable accurate tracking of the joint rotation of the human operator. Follow the principle of design there will be two attachments points for each link. Figure 3.6 depicts the locations of the attachment points of the master exoskeleton. The attachment method used here is the Velcro strap, which is chosen for its flexibility in length and its strength.

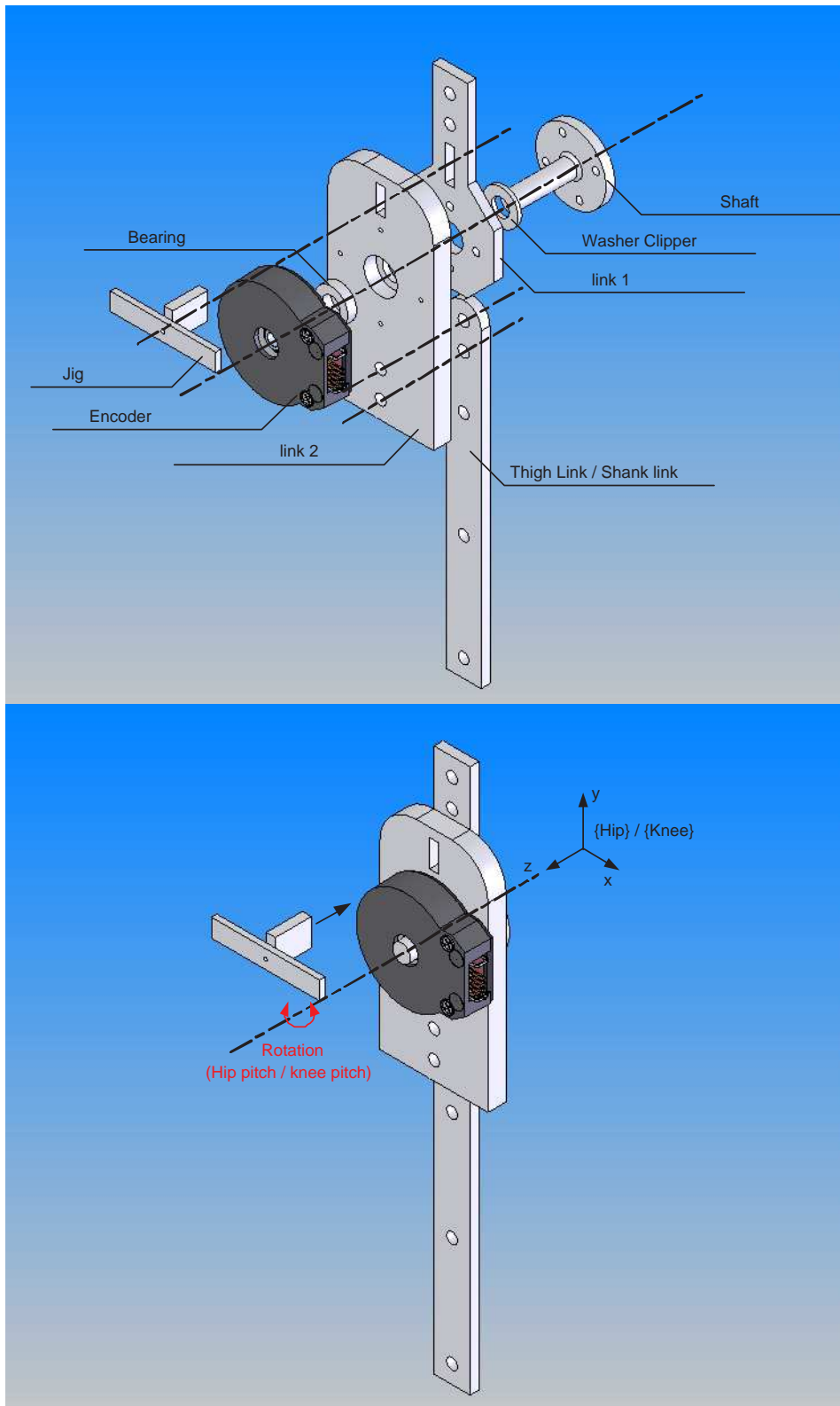


Figure 3.5: Top: Parts breakdown drawing for thigh/shank unit. Bottom: Illustration of the degree of freedom and coordinates of thigh/shank unit. Note the jig which can be inserted into the alignment slot for the purpose of initialization of the encoders.

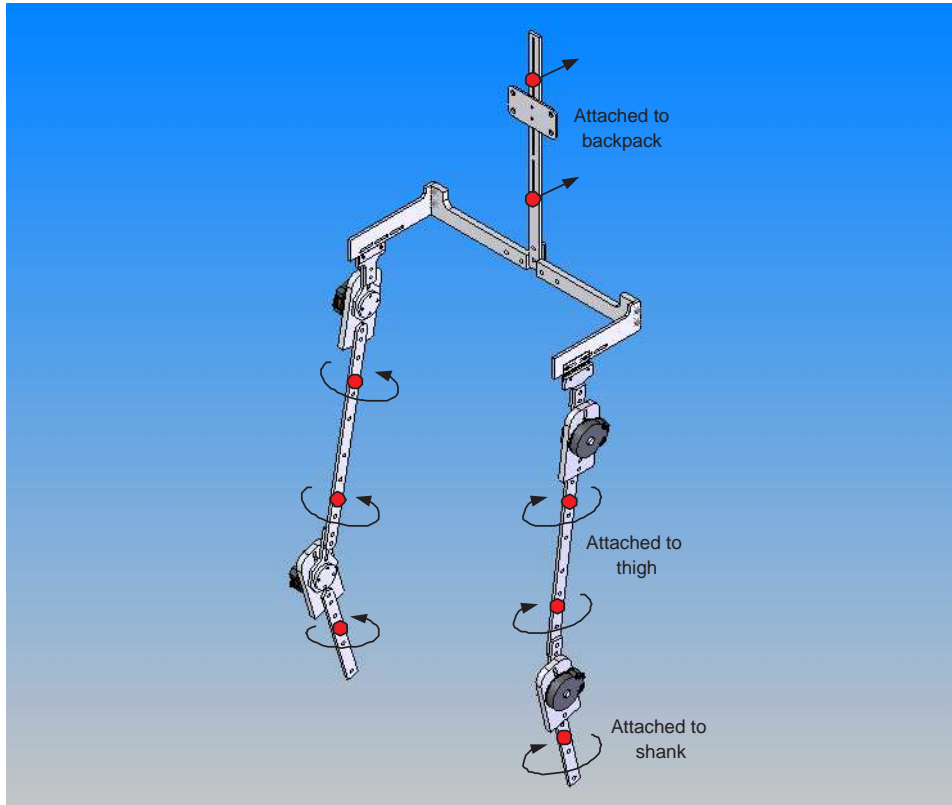


Figure 3.6: Attachment points of the master exoskeleton.

3.3 PC and Decoder Unit

The PC is used not only as an interfacing controller between master and slave, but also for the purpose of data collection. Important information such as the ZMP position (the stability indicator for the humanoid robot), the body tilt angle, and the visual and audio signals (indirect feedbacks) are all processed in the PC. The PC is a Pentium IV 2.0GHz with 256RAM. It runs on a Redhat 7.3 Linux OS (Kernel 2.4.18) with RTLinux kernel 3.2-pre1 to provide the real time environment for controlling the humanoid robot.

The decoder unit is made up of four HTCL2016 quadrature encoder counters and a common clock. The decoder unit is used to count the outputs of the four incremental encoders from the master exoskeleton, and produce a 16 bit digital output for the data acquisition card (National Instrument PCI-DIO-96). The clock speed is chosen to be 100 kHz so that it is capable of tracking human walking motion. Figure 3.7 depicts the schematic of the electronic circuit of the decoder unit.

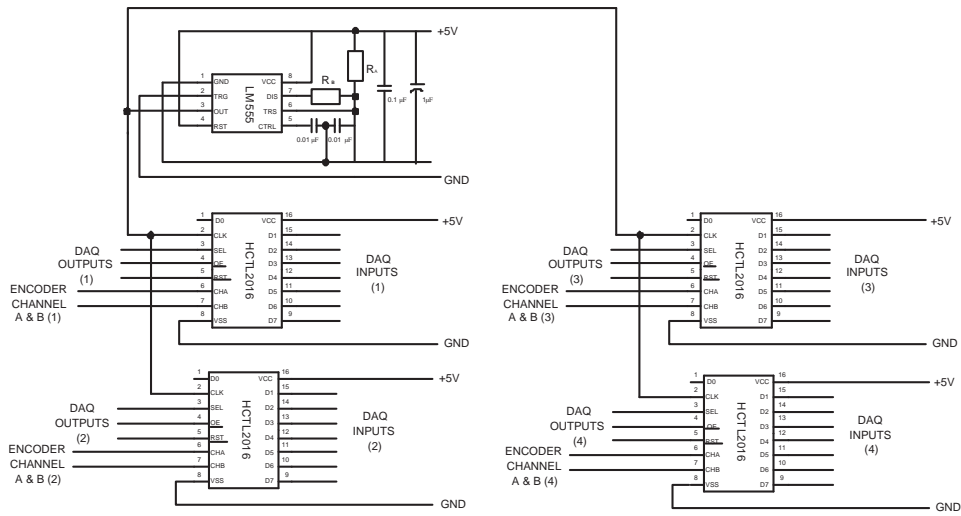


Figure 3.7: Schematic of the electronic circuit of the decoder unit.

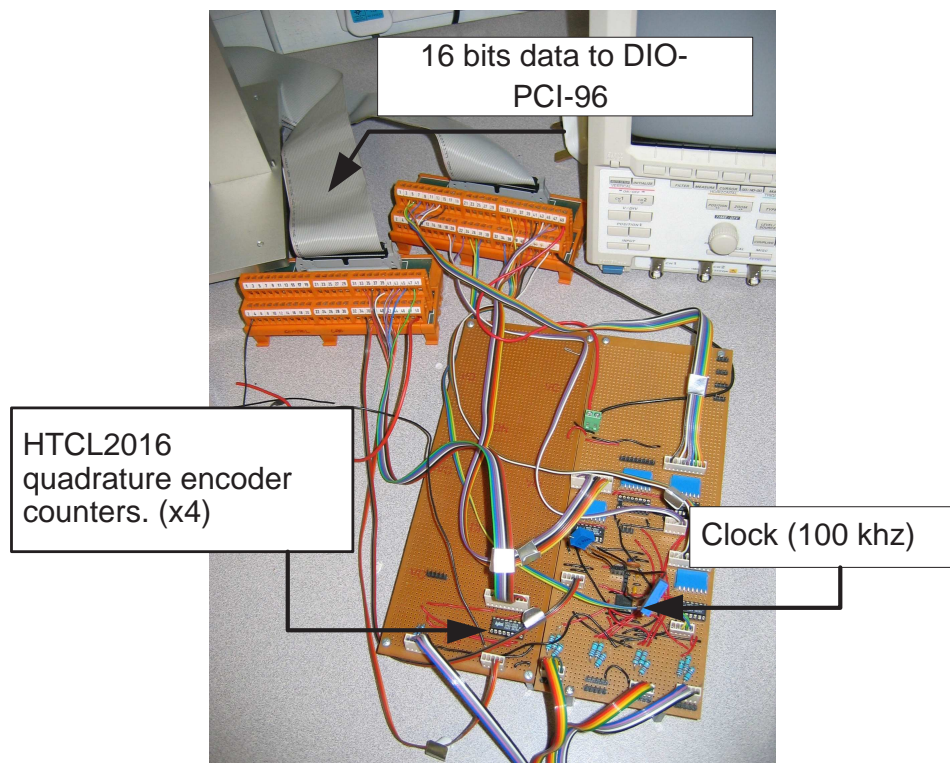


Figure 3.8: Decoder circuit.

3.4 Slave (Fujitsu Humanoid Robot HOAP-1)

The Fujitsu humanoid robot HOAP-1 is chosen as the slave for this teleoperation system. Two distinct advantages are first the robot is well designed and manufactured mechanical-wise; and second it gives the user a full information for the hardware and software interface.

The humanoid robot weighs 6kg and stands 48cm tall. It has a total of 20 Degree of Freedom (DOF) - 6 DOF each leg and 4 DOF each arm. The user-developed programs are designed to run on RT-Linux on an operating command PC, which communicates with the robot through a USB interface. The robot's internal sensors and actuators (motors) also use USB interface and can be easily expanded according to needs. Figure 3.9 illustrate the robot and its actuated degree of freedom (along with the designated coordinates).

To ensure the 2D locomotion of the humanoid robot, a support frame has been fabricated to restrict the frontal (sideway) movement of the robot. The robot is able to move freely in sagittal and transverse planes.

3.5 Optional Components

The optional components in the teleoperation system include a Head Mounted Display (HMD), a LED indicator and an audio speaker.

3.5.1 Head Mounted Display

Head Mounted Display (HMD) is included in the proposed teleoperation system for the purpose of future research on telepresence. HMD will provide video streaming in real-time, hence the human operator is able to see the surrounding of the robot; consequently a sense of "presence" in the remote site.

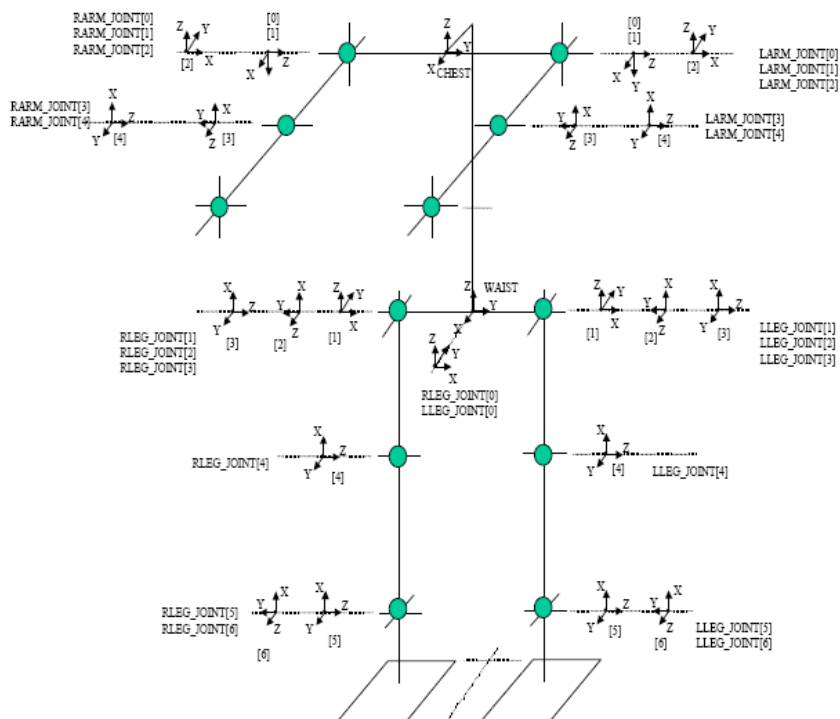
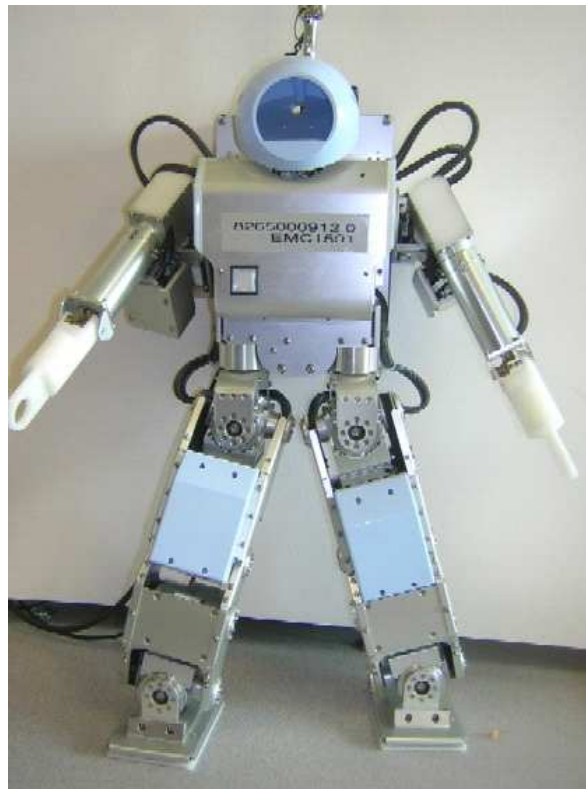


Figure 3.9: Top: Fujitsu HOAP-1 Humanoid Robot. Bottom: Joint coordinates of HOAP-1.

3.5.2 LED Indicator and Audio Speaker

These two components served the purpose of performance enhancement by providing an indirect feedback to the human operator. The improvement of performance in teleoperation by the aid of indirect feedback has been proven and demonstrated in some of the research. Hence the inclusion of these two components will certainly have the same effect.

The critical information that passes to the human operator in this teleoperation system is the ZMP information. As mentioned earlier in the Chapter 2, ZMP can be considered as a stability criteria for bipedal robot locomotion and hence the success of teleoperation. In real robot, ZMP can be monitored online by mounting force/torque sensors at the foot of the humanoid robot. It is possible that this information can be passed to the human operator either visually or in audio form.

In 2-D locomotion, a line of LEDs can be used to represent the discrete location of the ZMP on the foot of the robot. As for audio form of representing the location of the ZMP, one way is to introduce a sound where the loudness is proportional to the distance away from safety region, and high(low) pitch represent to the front(rear) of the foot.

Chapter 4

Kinematic Study

Preliminary study based on the biomechanics of human and human locomotion has been conducted to investigate the feasibility of the proposed control method. Static anthropomorphic measurement and joint range of both human and humanoid robot (HOAP-1) have been compared.

4.1 Static Anthropomorphic Measurement

In the field of biomechanics, a widely accepted conceptual model of human body is the "linkage-body" man. The name of linkage-body actually means the reference of the segments of the human body, by analogy with machines, as "linkages". As a result, data of human body parts, such as their dimensions and properties, are standardized for ease of research and study.

Since the project is focused on the teleoperation of humanoid walking, we are interested in the lower limb properties. Table 4.1 is the comparison table between human link length and the Fujitsu humanoid robot. The human data is adapted from (Pheasant et al., 1986), in accordance to the average stature of an adult Chinese. Two observations can be made immediately:

1. The percentile length of the thigh and shank of both the robot and the human is quite close.

2. The percentile length of the foot structure of the robot is much larger than human.

The percentile length is the ratio of link length and the stature height.

The first observation is somewhat expected as humanoids are designed to resemble human beings. Furthermore, one of the main purposes of building a humanoid is to be used as a research platform to understand human locomotion (Chew et al., 2003).

The reason for the second observation can be explained in terms of the stability and design constraint. The structure of the foot is made in such a way to increase the stability of the humanoid robot. Human has a lot more degree of freedom than humanoid robot, such as the flexible structure of the spine, and the toe on the foot. The lack of these extra degree of freedom results in the problem of balancing and hence the requirement of relatively large foothold for humanoid robot. In addition, the physical size of the DC motor, which is the main component of the joints, sometime compromise the design of the foot size of the humanoid robot.

The difference in the structure of the foot implied a potential problem if direct mapping of all the human joints is realized in the proposed teleoperation system. As the percentile length is larger for Fujitsu humanoid robot, it is foreseeable that the robot foot will interfere with the ground during the motion of toe off and heel strike. This can be rectified by regulating the ankle such that the foot is always parallel with the ground during walking. As the difference in foot structure can be resolved, we speculate that the direct mapping of the hip and knee joint in the teleoperation is feasible. Simulation result (Sim et al., 2004) has shown the viability of direct teleoperation of a humanoid with ankle regulation.

4.2 Joint Range

The second study focused on the joint limit of the Fujitsu humanoid robot. As sagittal plane walking is the focus for this research, only joint angles involved in the flexion and extension will be investigated. (Flexion movements are those which fold the body into the curled-up fetal position). The data of human here is adapted from the work of Damon (1966). It has been quoted extensively in the literature of biomechanics and

Table 4.1: Link length comparison between human and Fujitsu humanoid robot

	Human		Humanoid	
	percentile length	Length (mm)	percentile length	Length (mm)
Thigh	24.3	42.5	20.7	0.1
Shank	23.6	41.3	20.7	0.1
Foot	15.2	26.6	20.3	0.098
Ankle above sole	4.2	7.35	7.7	0.037
Ankle in front of heel	3.3	5.78	8.7	0.042

Table 4.2: Joint range comparison between human and Fujitsu humanoid robot

		Human	Humanoid
Hip	Flexion	113	70
	Extension	20	120
Knee	Flexion	125	120
	Extension	0	0
Ankle	Flexion	38	60
	Extension	35	60

ergonomic research.

Table A.1 is the comparison table of the joint range between human and Fujitsu humanoid robot. Human has a notably larger hip flexion compared to Fujitsu humanoid robot. This is a potential problem as during teleoperation, human operator is possible to issue a position command to the robot that is unachievable and consequently causing mechanical failure. As a result, soft limits have been incorporated in the control algorithm to avoid such incidents. As for the knee and the ankle, Fujitsu humanoid robot has either the same or larger joint range compared with human, no problem will occur.

Chapter 5

Control Methods and Dimensional Parameter Study

Two control methods have been identified to be implemented in the teleoperation system, namely direct mapping of joints , and mapping of foot positions (cartesian control). These two methods of teleoperation are done in real-time. Dimensional parameter study provide an approach that has the potential of further enhance the performance to the teleoperation system.

5.1 Direct Mapping of Joints

Direct teleoperation has long been the most common method in the control of tele-manipulators. The main advantage of this kind of control is its simplicity. Control block diagram of direct mapping of joints are illustrated in Figure 5.1.

The function of individual blocks are listed as followed:-

1. Human block - the only intelligent part of the whole system that has the function of sensing, decision making and action.
2. Master exoskeleton block - capturing the motion of human operator, the output of the block is the hip joint and knee joint.
3. Ankle regulation block - by taking hip and knee joint data as input, applying

algorithm to generate the ankle data such that the foot is always parallel with the ground.

4. Robot block - the slave robot that does work in the remote site.

5.2 Mapping of Foot Positions

The other control method is based on the idea of controlling the foot positions of the slave robot instead of all the joints. The foot is regarded as the end-effector in the case of tele-manipulation. The control block diagram is shown in Figure 5.2. This method is more complicated than the direct joint mapping method. Three extra control block is added.

The function of the additional blocks are listed as following:-

1. Forward kinematics block - take the hip and knee data as the input and calculate the foot position in cartesian space (x and y), with respect to hip.
2. Scaling and Modification block - the function of this block is to provide geometry scaling for the robot and modify the position of the foot to prevent the occurrence of singularities.
3. Inverse kinematics block based on the calculated foot position x_{mod} and y_{mod} , inverse kinematics algorithm is used to calculate the new hip and knee joint data.

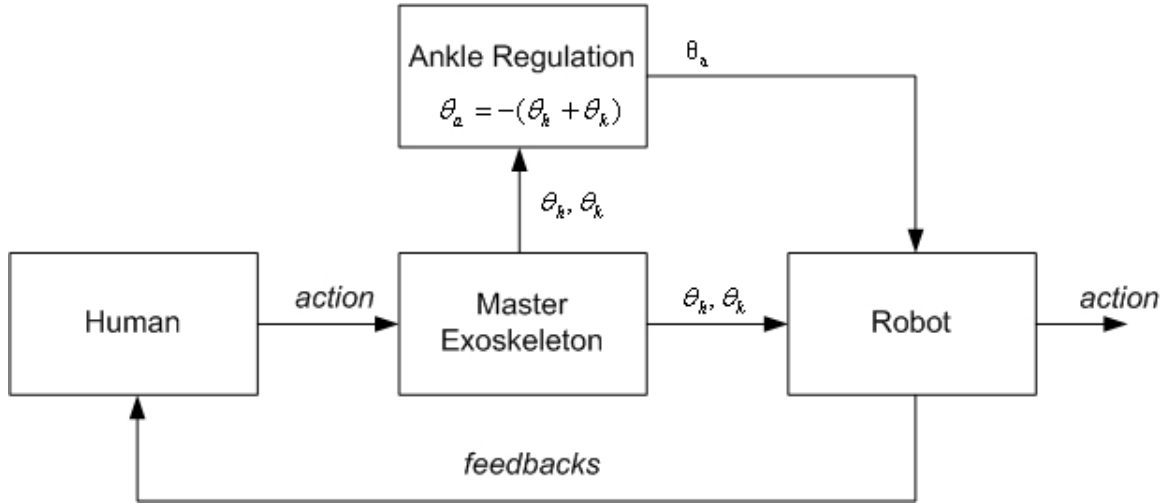


Figure 5.1: Control block diagram of the method direct mapping of joints

5.2.1 Forward Kinematics and Jacobian

In this section the forward kinematics of the master exoskeleton will be described. The Jacobian of the system will also be derived. The coordinate systems are defined for all the links of the master exoskeleton using Denavit-Harrtenberg convention(Craig, 2002). Frame attachment diagram is shown in Figure 5.3.

The base coordinate is located at the waist. Foot position of both swing foot and stance foot is calculated based on this base coordinate. The length of the thigh and shank are both fixed to L .

The Jacobian relates joint velocities to Cartesian velocities of the foot by the following relation:-

$$V = J \cdot \dot{\theta} \quad (5.1)$$

or vice versa, the joint velocities can be found by using the inverse of the Jacobian.

$$\dot{\theta} = J^{-1} \cdot V \quad (5.2)$$

The Jacobian can be derived by partial differentiation with the joint angles.

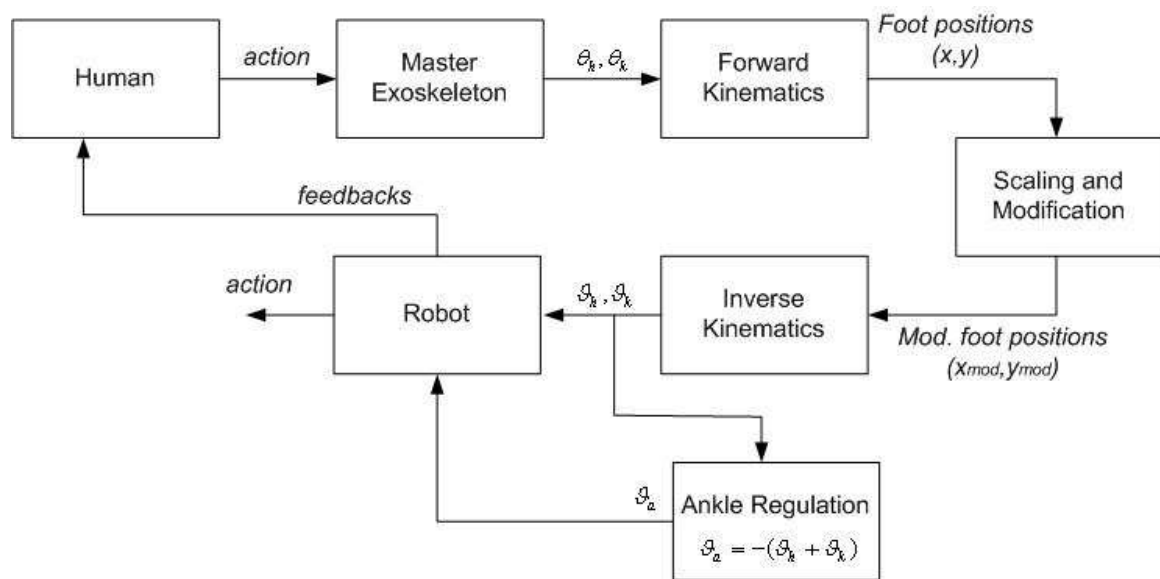


Figure 5.2: Control block diagram of the method mapping of foot positions

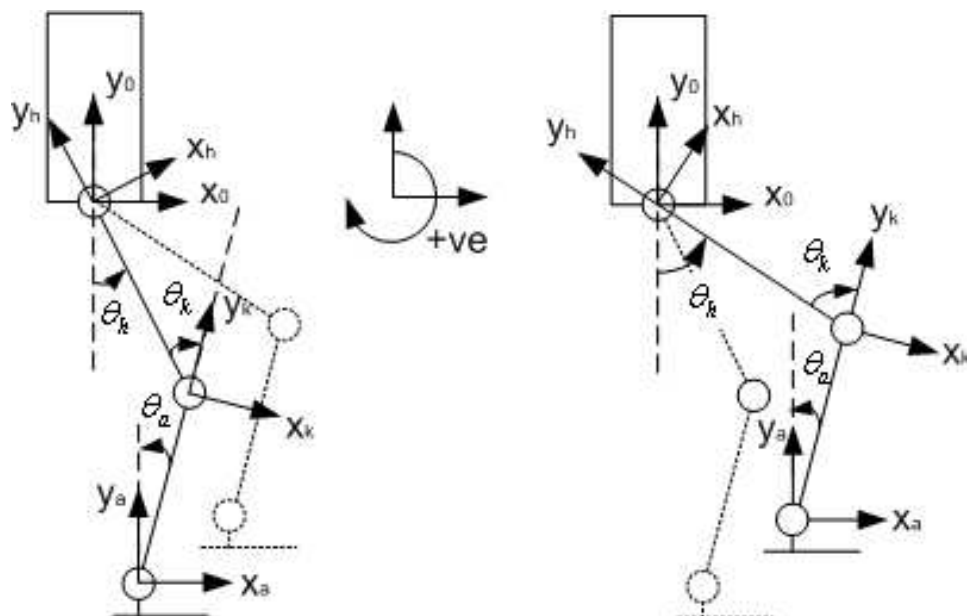


Figure 5.3: Frame attachment diagram for master exoskeleton. Left: Stance leg. Right: Swing leg.

$$J = \begin{pmatrix} \frac{\partial x_{master}}{\partial \theta_{hip}} & \frac{\partial x_{master}}{\partial \theta_{knee}} \\ \frac{\partial y_{master}}{\partial \theta_{hip}} & \frac{\partial y_{master}}{\partial \theta_{knee}} \end{pmatrix} \quad (5.3)$$

Subsequently, the Jacobian for the robot leg can be represented as:-

$$J = \begin{pmatrix} c_h + c_{h+k} & c_{h+k} \\ -s_h - s_{h+k} & -s_{h+k} \end{pmatrix} \quad (5.4)$$

where,

$$s_h = \sin \theta_{hip}, c_h = \cos \theta_{hip}, \text{ etc.}$$

From equation 5.1, it is obvious that the existence of the solution depends on whether the matrix J is invertible or not. The point where matrix J is non-invertible is called singularity point. In physical sense the robot loses its degree of freedom in singularity points, which will result in unpredictable behavior such as sudden change of robot configuration. As a result, it is important that the points of singularity (where the determinant of the matrix J equal to zero) are avoided in the operation.

$$\det J = \begin{vmatrix} c_h + c_{h+k} & c_{h+k} \\ -s_h - s_{h+k} & -s_{h+k} \end{vmatrix}$$

$$\begin{aligned} \det J &= L \cdot [-s_{h+k}(c_h + c_{h+k}) - c_{h+k}(-s_h - s_{h+k})] \\ &= L \cdot [-c_h(s_h c_k + s_k c_h) + s_h(c_h c_k - s_h s_k)] \\ &= -L \cdot s_k \end{aligned} \quad (5.5)$$

From equation 5.5, it is found that the singularity points occur at θ_{knee} equal to 0 or 180° .

5.2.2 Inverse Kinematics Transformation

This section will detail the inverse kinematics transformation that convert the foot position obtained from the master exoskeleton to the data in joint coordinates. The previous section showed that two possible singularities of the robot leg exist. One way to prevent the singularities is to modify the foot position such that the fully straighten configuration can be avoided. The method adopted here is to reduce the hip height (in other words, the vertical foot position) such that the robot is walking in a knee-bent fashion. Furthermore, the foot positions are also needed to be scaled down 25% due to the geometry difference of the human operator and the slave robot. The consideration of the 180° has been neglected as such configuration is not possible in normal locomotion.

The modified foot position are denoted as x_{mod} and y_{mod} respectively, while the joint angles for slave are denoted as ϑ_{hip} , ϑ_{knee} and ϑ_{ankle} respectively. L_{shank} and L_{thigh} are the length of the shank and thigh segments of the legs respectively.

The angle of the hip, knee and ankle of the slave can be calculated as below:-

Knee Joint:

$$\vartheta_{knee} = \arccos\left(\frac{y_{mod}^2 + x_{mod}^2 - L_{shank}^2 - L_{thigh}^2}{2L_{shank}L_{thigh}}\right) \quad (5.6)$$

Hip joint:

$$\vartheta_{hip} = \arccos\left(\frac{x_{mod} \sin \vartheta_{knee} + y_{mod}(1 + \cos \vartheta_{knee})}{\sin^2 \vartheta_{knee} + (1 + \cos \vartheta_{knee})^2}\right) \quad (5.7)$$

Ankle joint:

$$\vartheta_{ankle} = -(\vartheta_{hip} + \vartheta_{knee}) \quad (5.8)$$

5.3 Dimensional Parameter Study

The theory of dynamic similarity is well-known and very important in the study of animal locomotion. The theory (Alexander and Jayes, 1983) proposed that different size animals that moved in different speeds, may still move in a similar way. A classic example is the comparison between the locomotion of a mouse and a horse. A mouse may need to gallop in order to keep up with a walking horse, hence they move in a very different ways at their absolute velocity. However, their movements may be very similar in their preferred trotting velocity (their relative velocity).

Alexander and Jayes further defined six requirements for locomotion of animals to be considered dynamically similar:-

1. Geometric similarity - Linear dimensions of different-sized animals can be scaled by the same constant.
2. Similar phase relationships - Relative timing of limb movements during locomotion remains the same.
3. Similar duty factors - The ratio of the time for which the foot is in contact with the ground and the stride time remains the same.
4. Similar relative stride lengths - The distance between two consecutive ground contacts of the same foot normalized for leg length are equal for different sized animals.
5. Similar relative ground reaction forces - The ground reaction force upon the contact of the foot with the ground divided by the weight of the subject are equal for different sized animals.
6. Similar relative mechanical power output - The value of mechanical power output (the product of forces and velocities), which normalized to the weight of the animals are equal.

They hypothesized that these six requirements will be fulfilled if different-sized animals are travelled in the speed that translate to equal Froude number. This hypothesis

was tested by comparing the locomotion mechanics of different sized animals. They found that different size animals move in a very similar mechanics at equal values of Froude number. Although the same Froude number does not guarantee the dynamic similarity of running (Donelan and Kram, 2000), it works well with walking locomotion.

Froude number is a dimensionless parameter which is defined as the ratio between the inertia force and the gravitational force (Eq.5.9). As the mass of the leg cancel out each other in the numerator and denominator, it can be considered as a parameter that normalized the speed of locomotion using the gravity and the leg length (Eq.5.10).

$$Fr = \frac{mv^2}{L_{Leg}mg} \quad (5.9)$$

$$= \frac{v^2}{gL_{Leg}} \quad (5.10)$$

where v is forward velocity, g is gravitational acceleration and L_{leg} is the animals leg length (usually measured as height to hip).

The average ankle to hip length of an adult human is approximately 0.8m, whereas the humanoid robot used in this research project has an 0.2m ankle to hip length. By substituting the above dimensions into Eq.5.10, the theoretical (based on theory of dynamic similarity) walking speed of the humanoid robot equals to half the walking speed of the human (Eq.3 - Eq.6).

$$Fr = \frac{v_{master}^2}{gL_{Leg, master}} = \frac{v_{slave}^2}{gL_{Leg, slave}} \quad (5.11)$$

$$\Rightarrow v_{slave} = v_{master} \sqrt{\frac{L_{Leg, slave}}{L_{Leg, master}}} \quad (5.12)$$

$$= v_{master} \sqrt{\frac{0.2}{0.8}} \quad (5.13)$$

$$= 0.5v_{master} \quad (5.14)$$

A previous study (Sim, 2004) shows that based on the geometric scaling, the walking

speed of the humanoid robot is proportional to the link length of the limbs, i.e. the walking speed is a quarter of the human walking speed. Simulation result based on geometric scaling shows that the robot is able to walk successfully, albeit the stability margin of the result is limited.

The idea of a humanoid robot walking in a dynamically similar fashion is appealing to our research on teleoperation. However, the Froude number scaling method is based on theory of dynamic similarity which has been applied successfully on animals so far. The viability of applying Froude number scaling to our teleoperation system of humanoid will be investigated in simulation and detailed in the next chapter.

Chapter 6

Simulation

Simulation is done to further prove the feasibility of the proposed teleoperation system. The simulation will be divided into two major sections - geometric scaling method by simply playback the human walking profile, and Froude number scaling method by speeding up the playing back trajectories. For both simulations, sagittal plane walking in normal human walking speed is considered. Simulation software package used is "Yobotics! Simulation Construction Set" developed by Yobotics, Inc (Yobotics, web8). All the physical parameters of the robot used in the simulation are based on the Fujitsu Humanoid Robot HOAP-1 (Humanoid Open Architecture Platform) (HOAP-1, web7). As the geometry and mass distribution are different between human and humanoid robot, it is expected that human operator will have to change his gait in order to ensure stable motion for the humanoid robot. A few issues have been identified for future implementation based on real-time teleoperation using the master interface.

6.1 Mechanical Model and Control Method

Since the purpose of this simulation is to investigate the sagittal plane locomotion of the robot, the HOAP-1 humanoid robot is modeled as a 7-segment planar linkage. The head, arms and torso (HAT) are consider as a lumped mass attached to the legs. The remaining segments are thigh, shank and foot. The model has 3-DOF at the hip, knee and ankle joints for each leg. The joints are modeled as pin joints, with pure torque

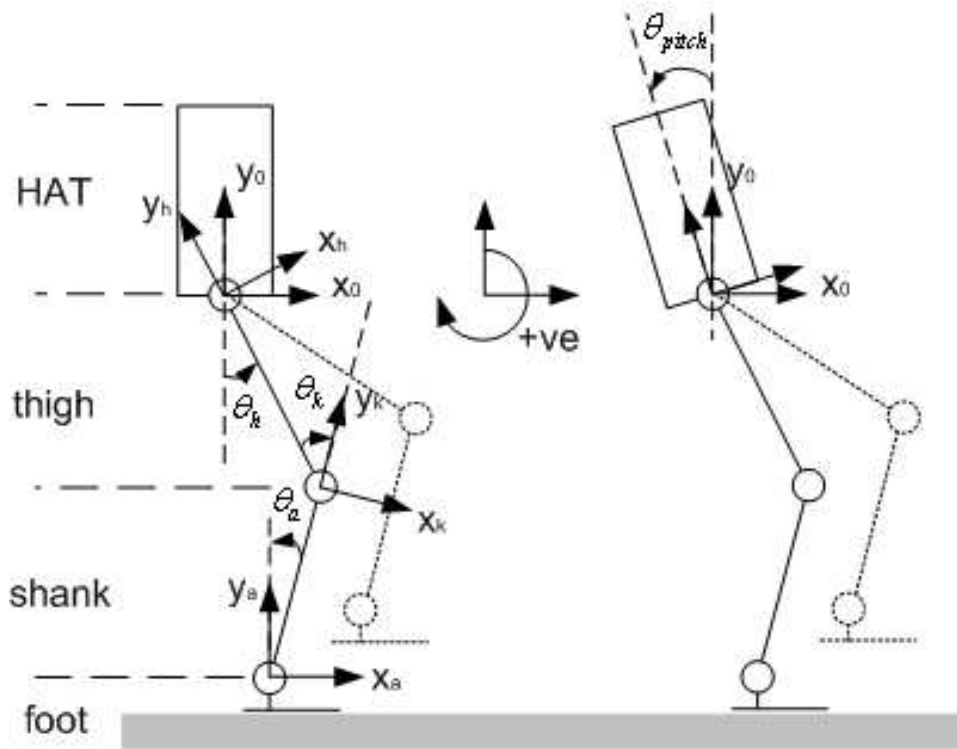


Figure 6.1: Mechanical model of Fujitsu humanoid robot HOAP-1. Left: Subscript h , k and a represent hip, knee and ankle respectively, while R and L represents right and left. Right: Body pitch angle.

generator. Mass and inertia properties for each linkage are used in accordance to the property sheet provided by Fujitsu Automation Co. Ltd. The mechanical model is shown in Figure 8. The physical attributes of the HOAP-1 used in the simulation are shown in Appendix A.

In the simulation, we use PD controller to generate the required torque for each of the joint trajectories.

$$\tau_{applied} = K_p(\theta_{ref} - \theta) + K_v(\dot{\theta}_{ref} - \dot{\theta})$$

where $\tau_{applied}$ is the torque generated by the joint, K_p and K_v are the position proportional gain and the velocity proportional gain respectively, θ_{ref} and θ are the reference and current joint angle, and $\dot{\theta}_{ref}$ and $\dot{\theta}$ is the reference and current angular velocity.

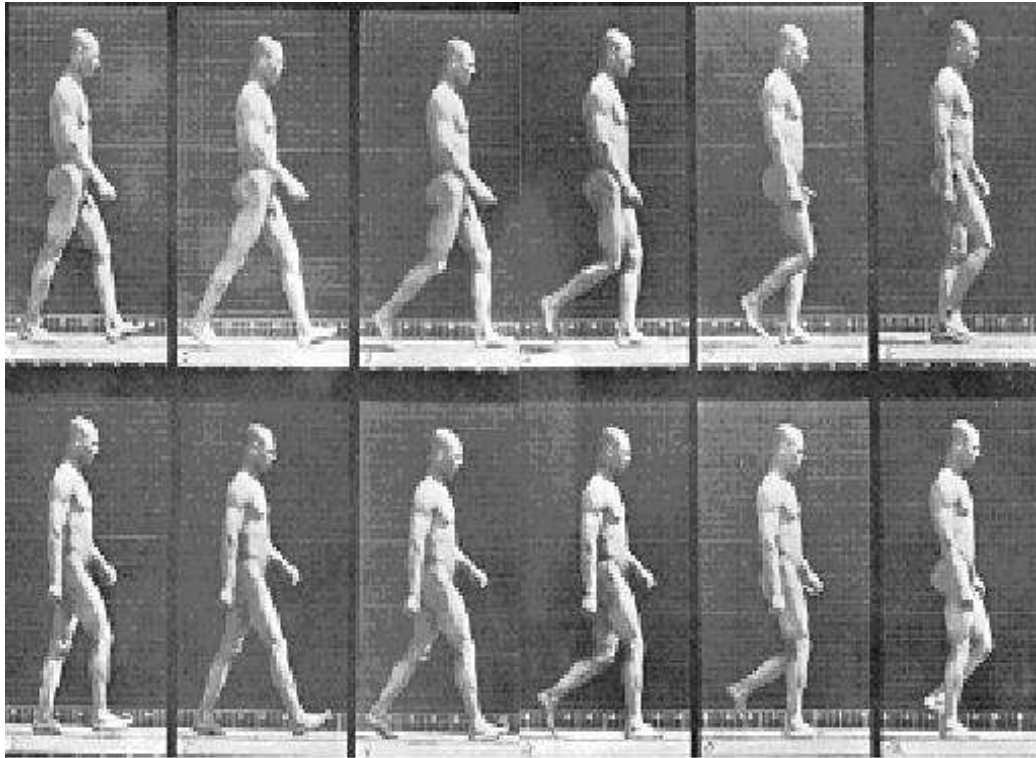


Figure 6.2: Man walking at normal speed. Muybridge (1955)

6.2 Joint Trajectory Acquisition

The human walking profile used in the simulation is obtained from the work of (Muybridge, 1955). Photos of a man walking in normal speed were used first for the purpose of simplification. The photos are shown in Figure 6.2. Hip, knee and ankle joint data were extracted from the photo in accordance with the configuration shown in Figure 6.1. The joints were then curve-fit as polynomial equations by using Least-Square Method. These polynomial equations are then entered as the trajectory equations of the joints in simulation. Once all the joint data are prepared, velocity profile needs to be generated such that PD controller can be implemented in the simulation. The velocity profile is the derivative of the joint trajectories.

6.3 Ankle Joint Data Modification

It is found that a potential problem is that the foot of the robot will interfere with the ground if the human walking profile is to be exactly executed by the robot. This is due to the fact that foot structure of the robot is different from the human. As shown in Figure 6.3 top, the heel of the robot is further away from the ankle, compared to the human (Nordin et al., 2001). In order to prevent this failure, the ankle data were modified such that the foot of the robot is always parallel with the ground. Refer to Figure 6.3 bottom, θ_{hip} , θ_{knee} and θ_{ankle} represent the angle of hip, knee and ankle joint respectively. By simple geometry, Equation 6.1 is used to generate the data for ankle, such that the foot is always parallel with the ground.

$$\theta_{ankle} = -(\theta_{hip} + \theta_{knee}) \quad (6.1)$$

6.4 Final Joint Trajectories

Least Square Estimation is used in the curve fitting to obtain the final trajectory of all the joints. The final joint trajectories used for the simulation are shown as followings:-

$$R_{hip} = (-28.674a^3 + 61.292a^2 - 40.268a + 8.0364) \quad (6.2)$$

$$R_{knee} = (-191.54a^4 + 582.62a^3 - 632.04a^2 + 287.65a - 46.634) \quad (6.3)$$

$$R_{ankle} = -(R_{hip} + R_{knee}) \quad (6.4)$$

$$L_{hip} = (71.054a^4 - 203.26a^3 + 208.95^2 - 92.348a + 15.276) \quad (6.5)$$

$$L_{knee} = (323.79a^5 - 1289.8a^4 + 2009.2a^3 - 1523.5a^2 + 560.06a - 79.813) \quad (6.6)$$

$$L_{ankle} = -(L_{hip} - L_{knee}) \quad (6.7)$$

where $a = s^*t$, s is the scale variable that control the playback interval, t is the playback time in the simulation.

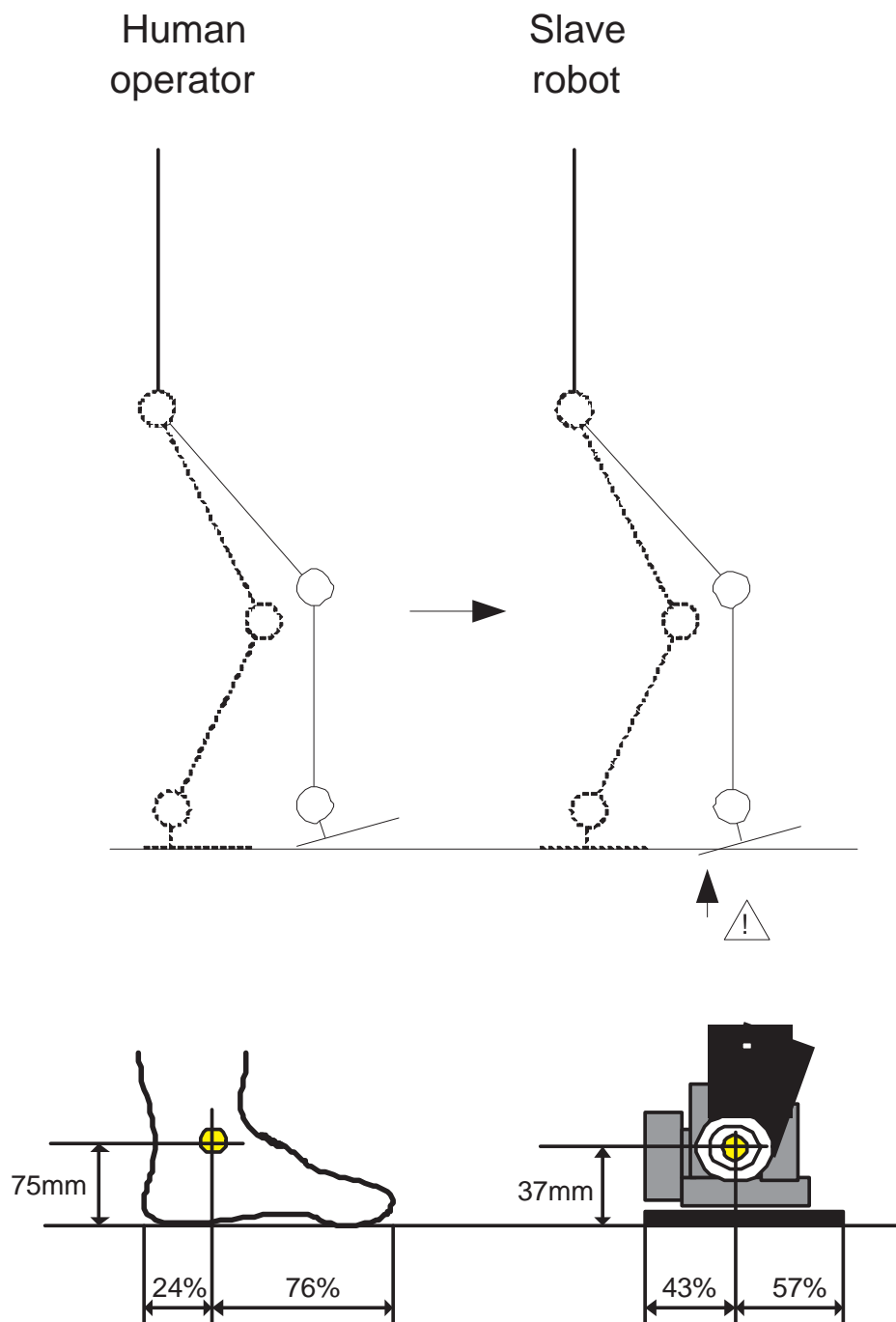


Figure 6.3: Top: Illustration of robot foot interfere with ground while playback the trajectory directly. Bottom: Comparison between human foot and robot foot. The ankle is the center of rotation.

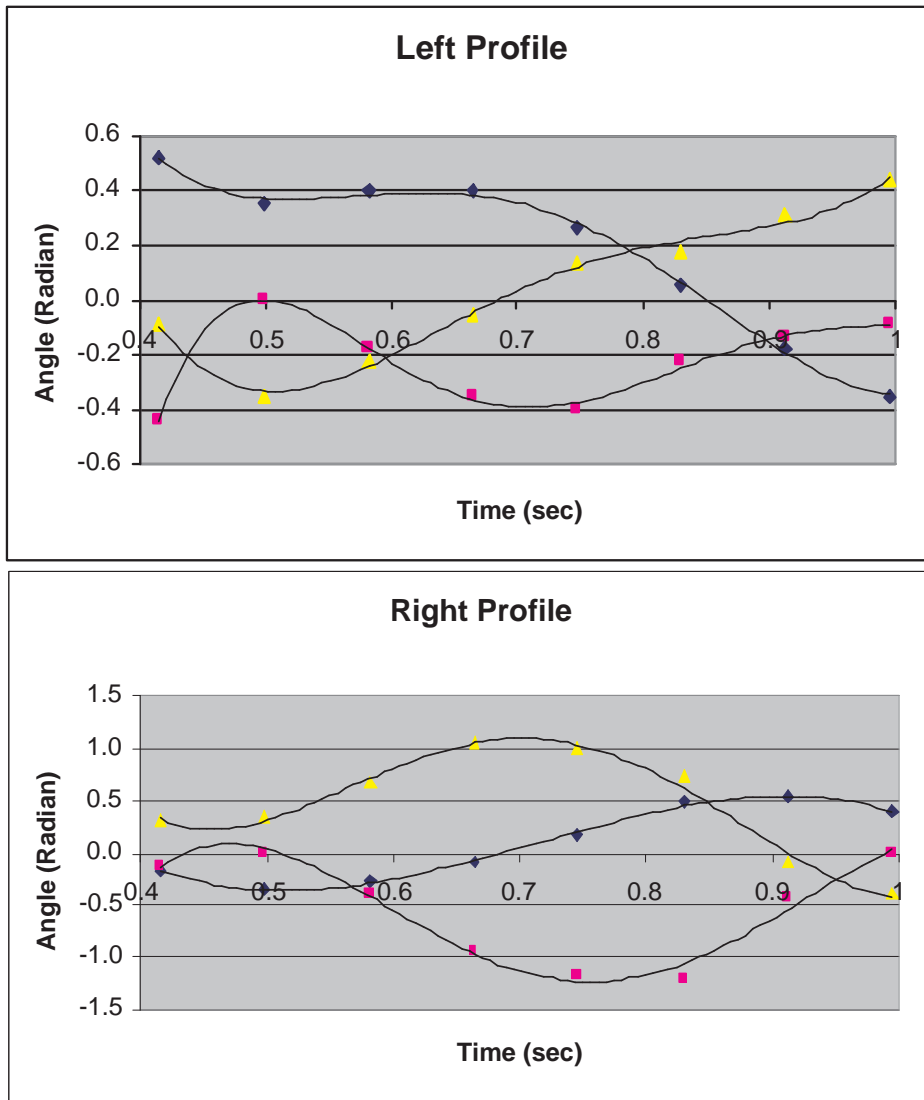


Figure 6.4: Top: Joint trajectories for left foot. Bottom: Joint trajectories for right foot. (Blue, yellow and magenta represents hip, knee and ankle respectively.)

The simulation is done by altering the variable s in the joint trajectories. As the joint trajectories are captured and estimated from a human walking at normal speed, a unity scale of the trajectories represents the case of geometric scaling ($v_{slave} = \frac{1}{4}v_{master}$). In order to realize half the human walking speed ($v_{slave} = \frac{1}{2}v_{master}$) for the case of Froude number scaling, the scale variable s is set to 0.5.

6.5 Model of the Ground

It is very difficult to model the ground exactly. In this simulation, we use non-linear spring linear damper to model the vertical behavior of the ground, while using linear spring damper to model the horizontal behavior. Using a nonlinear (hardening) spring in the vertical direction is a standard way to prevent ground chatter or bounce while still remains a stiff ground. The parameters of the ground are tuned such that an acceptable behavior - a trade off between ground penetration and bounce off of the robot, has been achieved.

6.6 Results of Geometric Scaling

For geometric scaling, we first investigate the overall walking behavior of the robot; then the landing impact of the locomotion.

6.6.1 Continuous Walking

As the mass distribution and physical attributes are different, it is expected that the robot will behave differently when the human walking motion is playback directly. The result of the simulation proved the feasibility of the proposed teleoperation system. After implementing the planned trajectory for simulation, the robot can walk a long time without falling, despite not being fully stable. Simulation was done for 10 minute for which the robot travels approximately 200m. The simulation snapshots for one gait cycle are shown in Figure 6.5.

During the locomotion, the robot is observed to be swinging periodically to the front and back, and also the support foot is not in full contact with the ground at all time. The main reason for this is due to the nature of the walking gait prescribed to the robot. The walking gait prescribed to the robot is a dynamic walking gait. The features of dynamic walking gait are large step length, high walking speed, and the center of gravity sometime goes outside the support foot. The fast movement of the links causing the dynamic effect (inertia forces of the links) plays a significant role in the overall

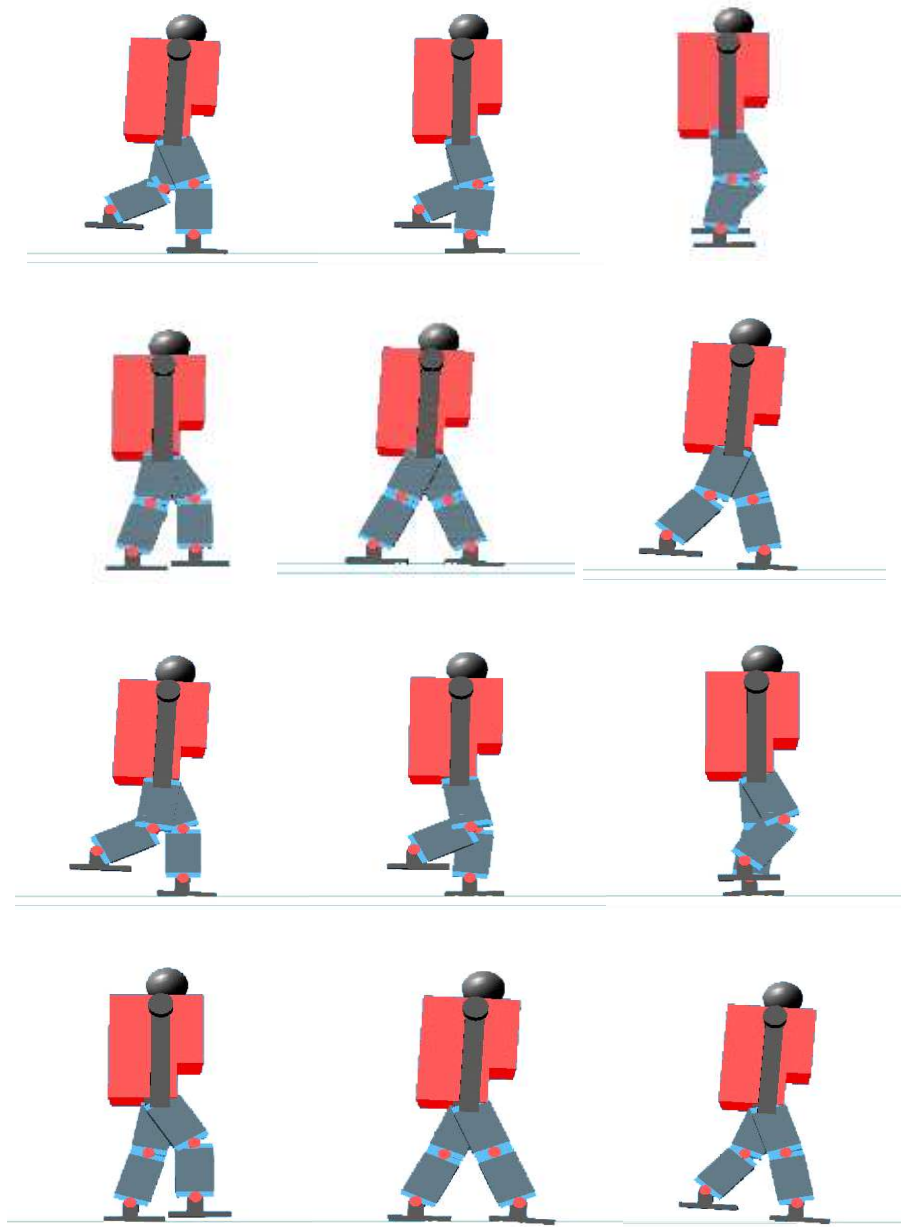


Figure 6.5: Snapshots for one gait cycle. Time interval is 0.083sec.

stability of the robot. As the dynamic of the robot is causing the support foot tipping towards the front; the landing motion of the swing foot is changed - Instead landing the swing foot flatly on the ground, the swing foot is now landing the ground toe on.

6.6.2 Landing Impact

The landing impact not only has a direct influence on the stability of the robot, but also affects the life of the mechanical parts of the robot. During locomotion, each landing action causes the occurrence of the impact. It is predictable that this frequent occurrence of landing impact will have a devastating effect on the mechanical parts of the robot.

By general physics, we know impulse-momentum change theorem is governing the behavior of the impact. Impulse-momentum change theorem states that the impulse experienced by an object is always equal to the change in its momentum. In terms of equations, it can be expressed as:-

$$f \cdot t = m \cdot \Delta v \quad (6.8)$$

where, f , t , m and v represents force, time, mass and velocity respectively.

Figure 6.6 show the value of the ground reaction force upon landing is taken place. Result shows a large impact force occur upon landing of the swing foot. The robot weight 6kg (60N). The maximum landing impact force detected in the simulation is found at approximately 6 times larger than the robot weight. This indicates the potential risk of damaging the mechanical structure of the robot, if the robot is teleoperated by normal human walking speed.

6.7 Result of Froude Number Scaling

Results included in this section are the analysis of body pitch and the ZMP profile. As human walks in an upright fashion, it is natural to choose body pitch as one of the key elements to evaluate the humanoid locomotion. The other key element - ZMP is widely used as a criteria to evaluate the stability of biped locomotion. Generally speaking, if

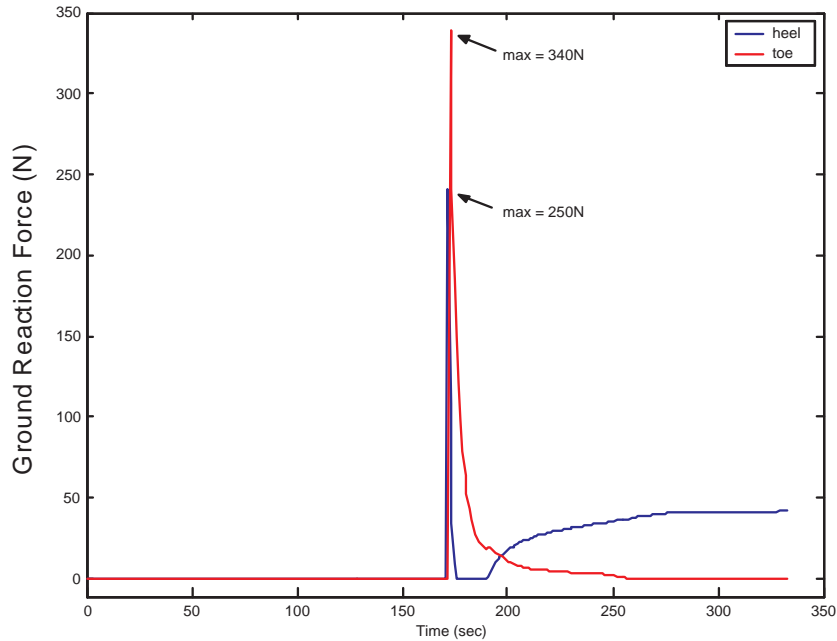


Figure 6.6: Ground reaction force of swing foot after landing. Blue and red represents data for heel and toe respectively.

the ZMP remains to be within the foothold, stable bipedal locomotion can be achieved.

6.7.1 Body Pitch

It is observed that the rocking of the robot happens regardless the scaling methods. Body pitch angle is measured in accordance to Fig.6.1 (Right). Table 1. is the comparison of the body pitch profile between two scaling methods. Fig.6.7 depicts the body pitch profile of the two scaling methods. Several observation is listed below and detailed deductions from these observations will be discussed in section 6.9.:-

1. The range of body rocking decrease 38% from a range of 5.9° for geometric scaling, to 3.7° for Froude number scaling.
2. The robot exhibit a more "balance" rocking motion for Froude number scaling (1.8° forward and backward); compare to geometric scaling (4.3° forward and 1.6° backward).
3. The frequency of the body rocking remains the same regardless of the scaling

Table 6.1: Comparison of body pitch profile between geometric scaling method and Froude number scaling

	Geometric	Froude
max	1.6° (0.028 radian)	1.8° (0.031 radian)
min	-4.3° (-0.075 radian)	-1.8° (-0.031 radian)
range	5.9° (0.103 radian)	3.6° (0.063 radian)

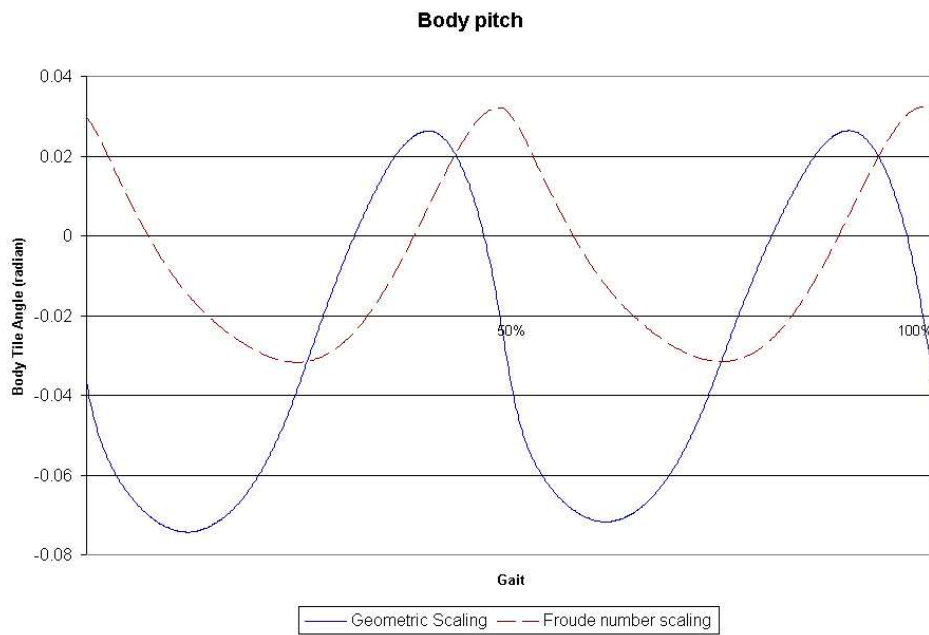


Figure 6.7: Comparison of the body pitch profile between kinematic scaling method and Froude number scaling method. The plot depicts the body pitch in one gait cycle.

methods.

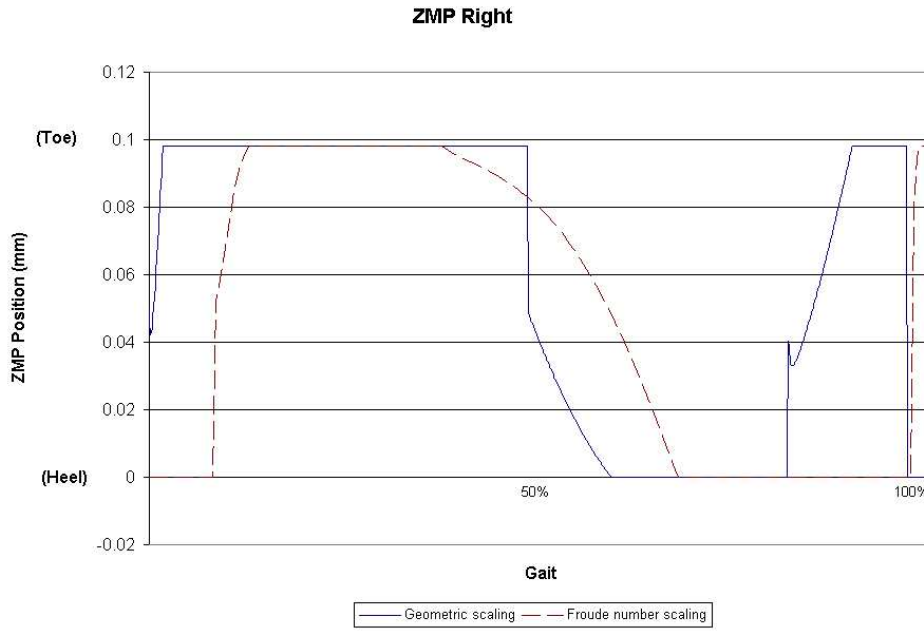


Figure 6.8: ZMP profile of right foot during right stance phase of the gait cycle. This profile is plotted against the time of right stance phase. The y-axis value of 0 represents ZMP is located at the heel, whereas 0.098 represents toe.

6.7.2 Zero Moment Point

Zero Moment Point (ZMP) is widely used in the field of biped locomotion as a stability criteria. In order to maintain balance during locomotion, ZMP should be maintained in the support polygon. Fig.6.8 and Fig.6.9 shows the ZMP profile of right foot and left foot during their stance phase respectively. Regardless of the scaling, ZMP always goes to the edge of the foot (either toe or heel) at some stage of the gait.

The percentage time of ZMP stays at the edge of the foothold ($T_{percentage}$) has been calculated in order to compare the stability of two cases.

$$T_{percentage} = \frac{T_{edge}}{T_s} * 100\%$$

where T_{edge} is the total time ZMP stays at the edge of the foot, and T_s is the stride time.

For geometric scaling, 37% of the stride time ZMP stays at the edge of the foot, while for Froude number scaling is 32%. In other words, there is an increase of 5% time

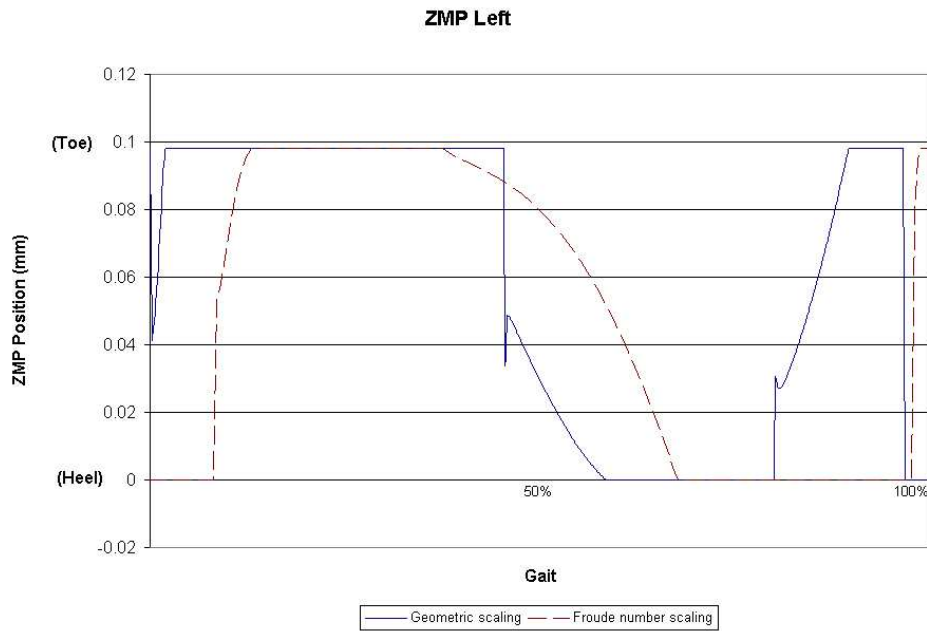


Figure 6.9: ZMP profile of left foot during left stance phase of the gait cycle. This profile is plotted against the time of left stance phase. The y-axis value of 0 represents ZMP is located at the heel, whereas 0.098 represents toe.

the ZMP stays within the foothold for the case of Froude number scaling.

Another interesting point is the rate of movement of the ZMP. Unlike the sudden shift of ZMP from toe to heel (and vice versa) for the case of geometric scaling method, the ZMP profile of Froude number scaling shows a more gradual movement of ZMP. In the case of human walking, the ZMP move from heel to toe gradually as the swing foot move from back to the front, until double support phase is reached. A more gradual movement of ZMP not only results in a more stable bipedal locomotion, but also reflect that the humanoid robot is walking in a more dynamically similar way as human.

6.7.3 Gait Phases

There are three phases in bipedal locomotion - left swing, right swing and double support. Fig.6.10 is the phase diagram of the simulation. It is clear that the difference between the normal human walking profile and the rest is the time of the double support phase. The normal human walking profile has a 33% double support phase compare with the instantaneous double support phase of the foot regulated profile. The foot reg-

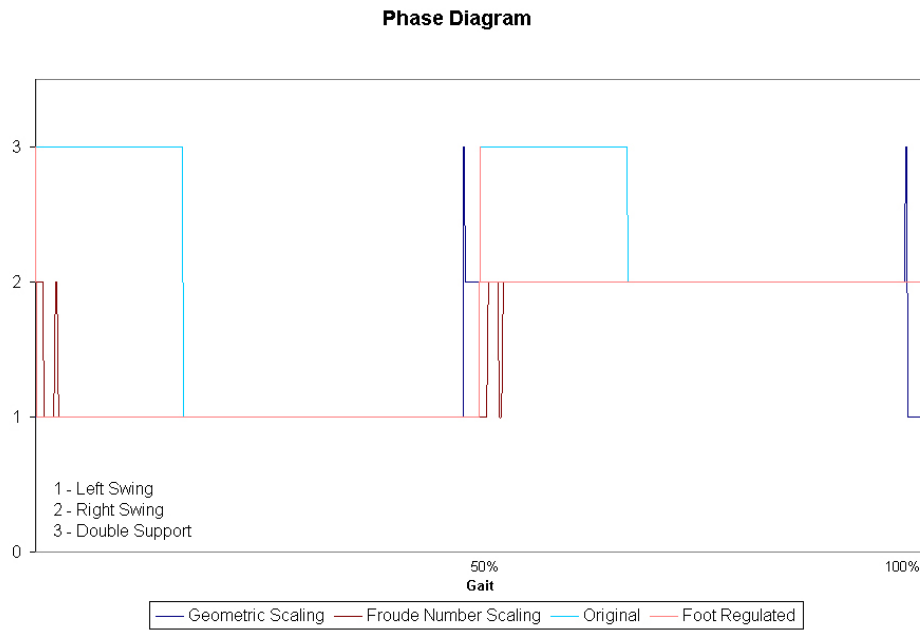


Figure 6.10: Phase comparison between normal, foot regulated, and scaled simulations.

ulated trajectories change the duty factors of the original human walking profile - which is one of the criteria of dynamic similarity of locomotion. Hence it is expected that dynamic similarity of the locomotion will be changed.

6.8 Discussion of Simulation Results

Based on the simulation results, we can verify the feasibility of the proposed control scheme and identify issues that will affect the implementation of the real teleoperation system. From the simulation of direct playback of the human trajectories, direct control of the ankle joint is unnecessary. As a result, the ankle trajectory needs to be modified such that the foot is always parallel with the ground to prevent interference. This finding directly affects the design of the master interface and the control scheme proposed.

From the simulation of the playback modified trajectories, we observed that when the walking motion is fast, the dynamics effect plays a significant role in the locomotion, which makes the balancing of the robot a difficult task. Even if the robot achieves locomotion under the normal human walking speed, the locomotion is marginally stable. Marginally stable also means that any small changes in robot itself or the environment

will certainly cause the robot to fall. Based on this result, slow walking motion for teleoperation is recommended.

The result of the landing impact shows that the maximum impact force is 6 times larger than the average force applied on the foot during the landing of the swing foot. Referring to Equation 6.8, we can either increase the time of impact, or decrease the change in velocity in order to minimize the impact. One way of increasing the time of impact is to attach some kind of impact absorption mechanism at the foot sole of the robot. For example, Honda Asimo (Hirai, 1998) realized this by having rubber bushes inserted into a guide just above the rubber foot sole. The rubber bushes deform elastically in the vertical direction upon a force being transmitted from the sole. As for the second method of minimizing the impact, we can control the landing motion of the swing foot. By slowing down the landing motion of the swing foot, the impact can be reduced.

To summarize, the feasibility of proposed teleoperation system is verified in the simulation - the robot is able to walk, despite being marginally stable, by simply playback the human normal walking profile. The simulation findings also provide an insight of the real system - despite the mechanical differences between master and slave, the proposed system will work if:

1. The ankle needs to be regulated to prevent interfering with the walking surface during swing phase.
2. The human operator can perform teleoperation slower than normal walking speed to prevent instability due to the dynamic effect. This also reduces the landing impact.

The Froude number scaling result is conducted to find out whether the stability margin will be improved as a result of applying Froude number scaling based on the theory of dynamic similarity. Although Froude number scaling results in a faster walking speed than the geometric scaling method, the results shows marginal improvement in terms of body posture and ZMP profile. The result of body pitch profile shows improvement after applying Froude number scaling. Not only the rocking of the body decrease 38%

to a range of 3.6° , but also the rocking motion is now more "balance" in the sense that forward and backward movement are the same (1.8°). The ZMP result shows an increase of 5% gait time which the ZMP stays within the foothold for the case of Froude number scaling. A more gradual movement of ZMP is also observed for the case of Froude number scaling.

Although the improvement of the Froude number scaling over geometric scaling is slight, and most importantly the stability of the locomotion is not 100% guaranteed, one crucial factor - duty factor of the gait, must not be overlooked in this study. By regulating the foot trajectory, the duty factor of the gait is changed, hence the dynamic similarity is lost between the two even with the same Froude number. Future study should look deeper into this aspects, either by controlling the foot height of both feet during double support phase; or changing the human landing foot posture - land flat in order to eliminate the heel strike and toe off action.

Chapter 7

Experimental Results

Five experiments have been conducted in order to test the teleoperation system. The first experiment is conducted for the purpose of evaluation of the hardware design. The second experiment tests the method of direct mapping of joints. The third experiment tests the control method based on the foot position. The fourth and fifth experiments are conducted to investigate the viability of reducing the walking speed or walking profile of the humanoid robot during the teleoperation.

7.1 Experiment 1 - Stepping

The first experiment for hardware evaluation is the stepping experiment. Evaluation of the master exoskeleton is the focus of this experiment. The human operator task is to step four times at the same spot: left-right-left-right. The knee is purposely flexed inwards to make sure, by intuition, to keep the center of pressure within the support foot.

In the first few trials, two major hardware design problems were observed. As the shank portion of the exoskeleton is shorter, there can be only one Velcro strap to strap onto the shank of the human operator. After the stepping motion, the shank link tends to slip away from the correct position. Also relatively small size of the shank makes the rigid linkage follow the thigh motion hence result in a disparity of the shank linkage with human operator's shank.

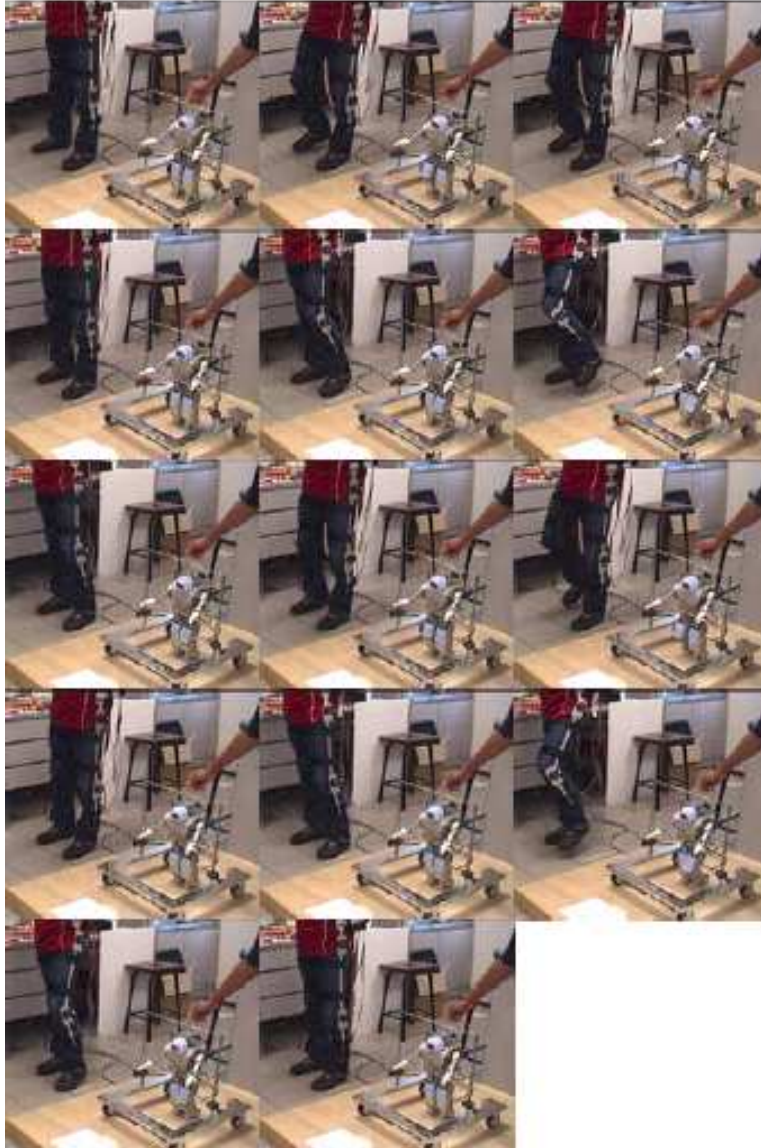


Figure 7.1: Snapshots of the stepping experiment. Snapshots are taken in the time interval of 1 second. (From left to right, top row to bottom row)

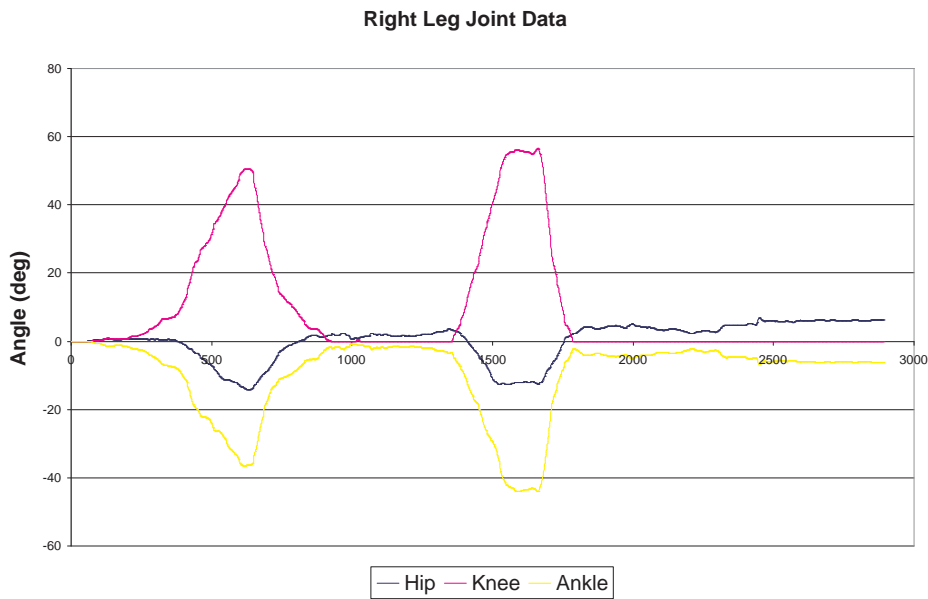


Figure 7.2: Right leg joint trajectories. Blue: Hip; Magenta: Knee; Yellow: Ankle.

In order to solve the first problem mentioned, a sponge-like material was added around the strap to provide a firmer grip. After the modification, the shank link is moving well with human operator’s shank. Further improvement is expected when the shank portion of the master exoskeleton is lengthened to accommodate two velcro strap.

The result shown here is the successful trial after the modification mentioned above. The foot is purposely regulated such that it is always parallel with the level ground. The snapshot of the experiment (Figure 7.1) verifies the foot regulation and also the effectiveness of the teleoperation system.

Figure 7.2 and Figure 7.3 are the joint trajectories for this stepping experiment. Figure 7.4 is the ZMP plot of the experiment. The ZMP value is calculated based on the force sensors data acquired from the robot. The ZMP plot of the stepping experiment shows that at the end of the stepping motion, the ZMP actually move closer to the toe. This is expected as from the joint data recorded, the human operator did not maintain an upright posture at the end of the experiment (approximately 8 degree). According to the experiment done before, the maximum hip flexion and extension in a static standing position for the humanoid before ZMP stays in the boundary of the foot sole are 10 degree respectively. Hence the experiment result agreed with the result obtained before.

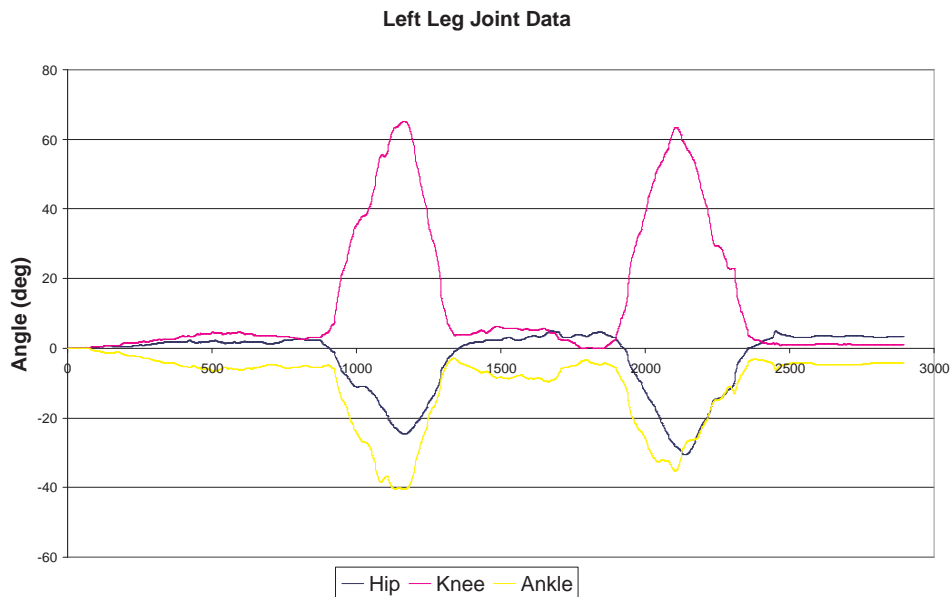


Figure 7.3: Left leg joint trajectories. Blue: Hip; Magenta: Knee; Yellow: Ankle.

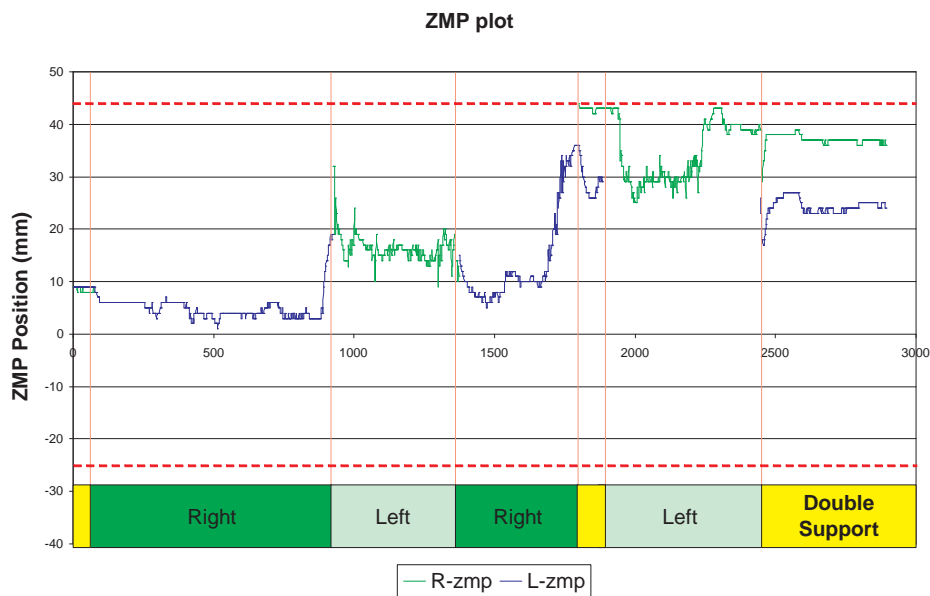


Figure 7.4: ZMP history for the stepping experiment. The red dash lines are the limit for the ZMP value, which is maximum +43 and minimum -26. ZMP for right and left foot are represented in yellow and turquoise lines respectively. The boxes at the bottom of the graph are the state of the humanoid robot - bright green: right foot lifted; light green: left foot lifted; yellow: double support.

7.2 Experiment 2 - Direct Mapping of Joints

The objective of this experiment is to investigate the performance of the first control method - direct mapping of joints from master to slave. The task of the human operator is to control the humanoid robot to walk 5 steps from a standstill position, and at the same time try to maintain the balance of the robot. The human operator will be told the critical information - normal walking motion and big step will certainly result the fall of the robot. Figure 7.5 shows the walking sequence of the direct teleoperation experiment.

One of the major finding of the result is that even the human operator walk in a extremely careful manner - small steps and slow motion, the robot will exhibit instability at the instance of transition from single support to double support. This is due to the indirect control of the ankle joint of the robot. The ankle is regulated such that the orientation of the foot is always parallel with the ground, however this introduce a difference in the timing of touch down. Besides, the error of the angle positions due to the disparity between the master exoskeleton and the human operator cannot be fully prevented. Figure 7.6 illustrate the difference of the landing timing of the swing foot which cause the robot to fall.

Such a problem can be resolved by asking human operator to walk in an unnatural fashion such that both feet remain parallel with the ground. Nevertheless, this is undesirable because this approach increase the mental burden of the human operator. As a result, the human operator will fatigue and get tired quickly.

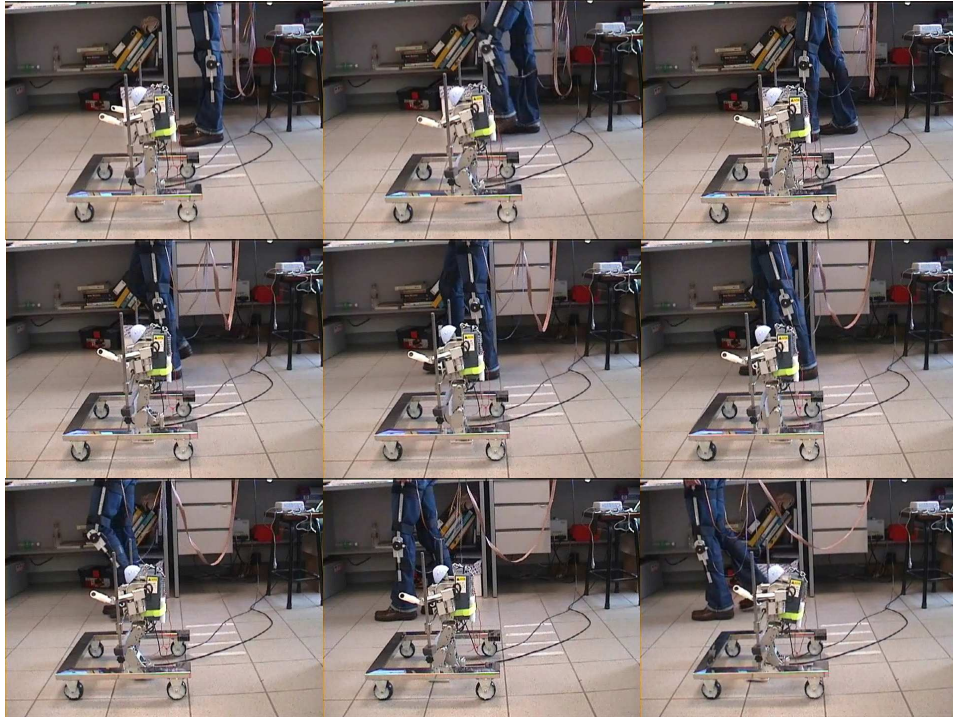


Figure 7.5: Walking sequence of direct teleoperation. The humanoid robot shown instability during landing of swing foot and eventually fall at the second step.

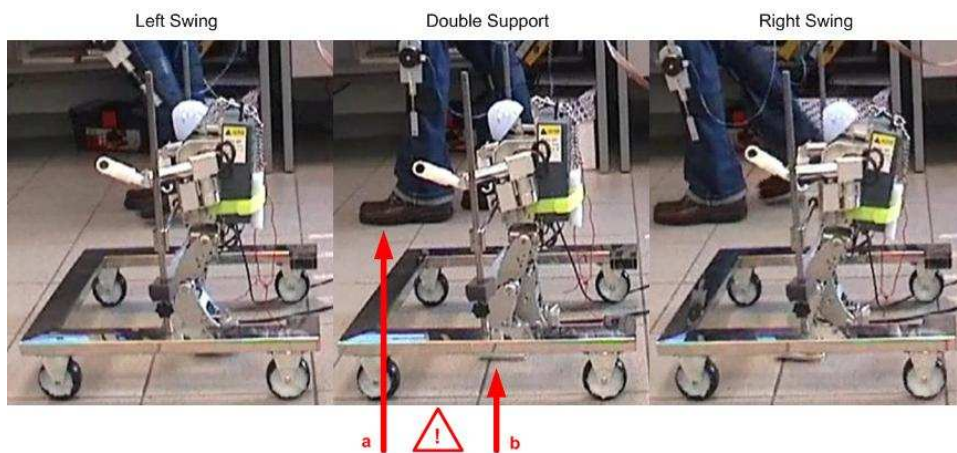


Figure 7.6: Illustration of the difference in timing for the landing of the swing foot. Arrow-a: Human operator has landed his swing foot. Arrow b: Left leg of the humanoid robot is yet to land.

7.3 Experiment 3 - Mapping of the Foot Position

The second control method is based on the mapping of the foot position. The humanoid robot is controlled such that the foot position is to follow the master's, instead of all the joints.

The result is promising as the landing of the foot is significantly more stable than the method of direct mapping of joints. In this experiment, human operator seems more comfortable and confident than the previous experiment. Simplification of the task is the reason for this change. Instead of all the leg joints, simply controlling the foot position (foot height and stride length) to achieve locomotion is a simpler task. Leg configuration is not critical as this experiment is essentially controlling the foot position to achieve locomotion.

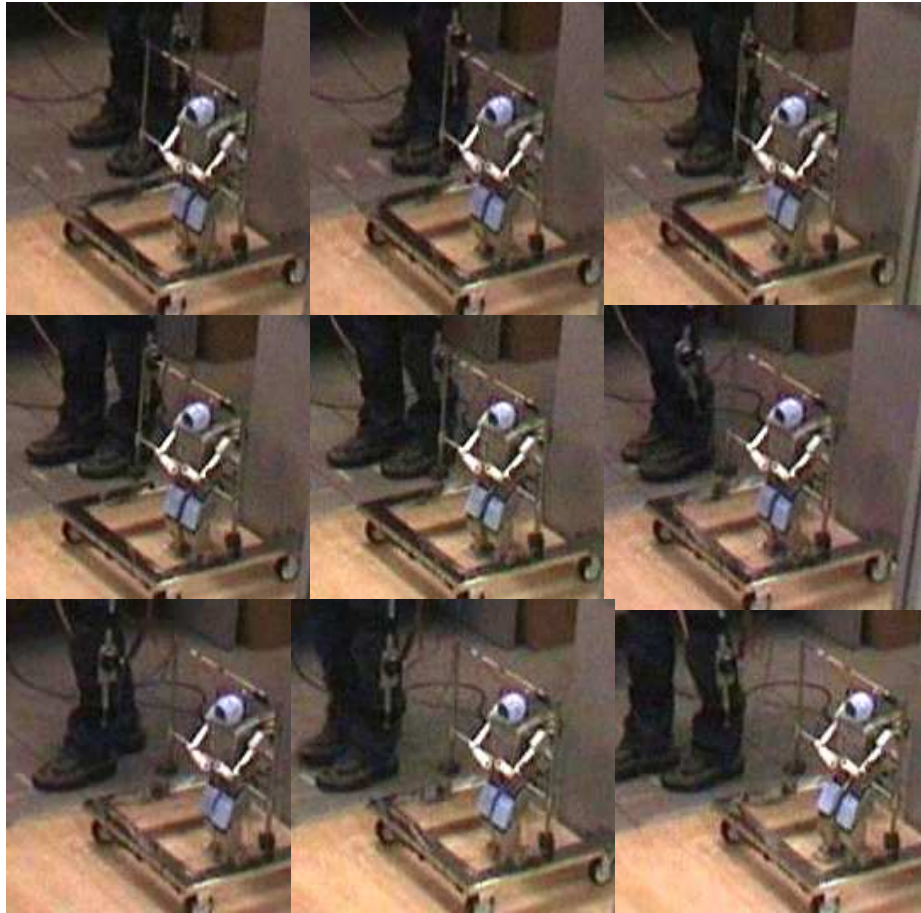


Figure 7.8: Walking sequence of the humanoid. Notice the first snapshot, the knee of the humanoid robot is bent even human operator is stand with straighten knee. This is a measure to prevent singularities in the Inverse Kinematic algorithm.

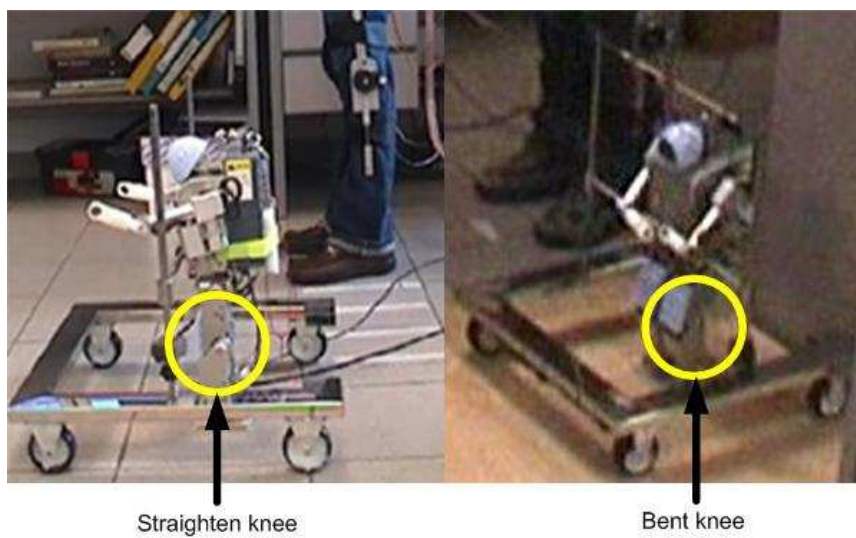


Figure 7.9: Comparison of the knee configuration of Direct joint mapping method and Foot mapping method.

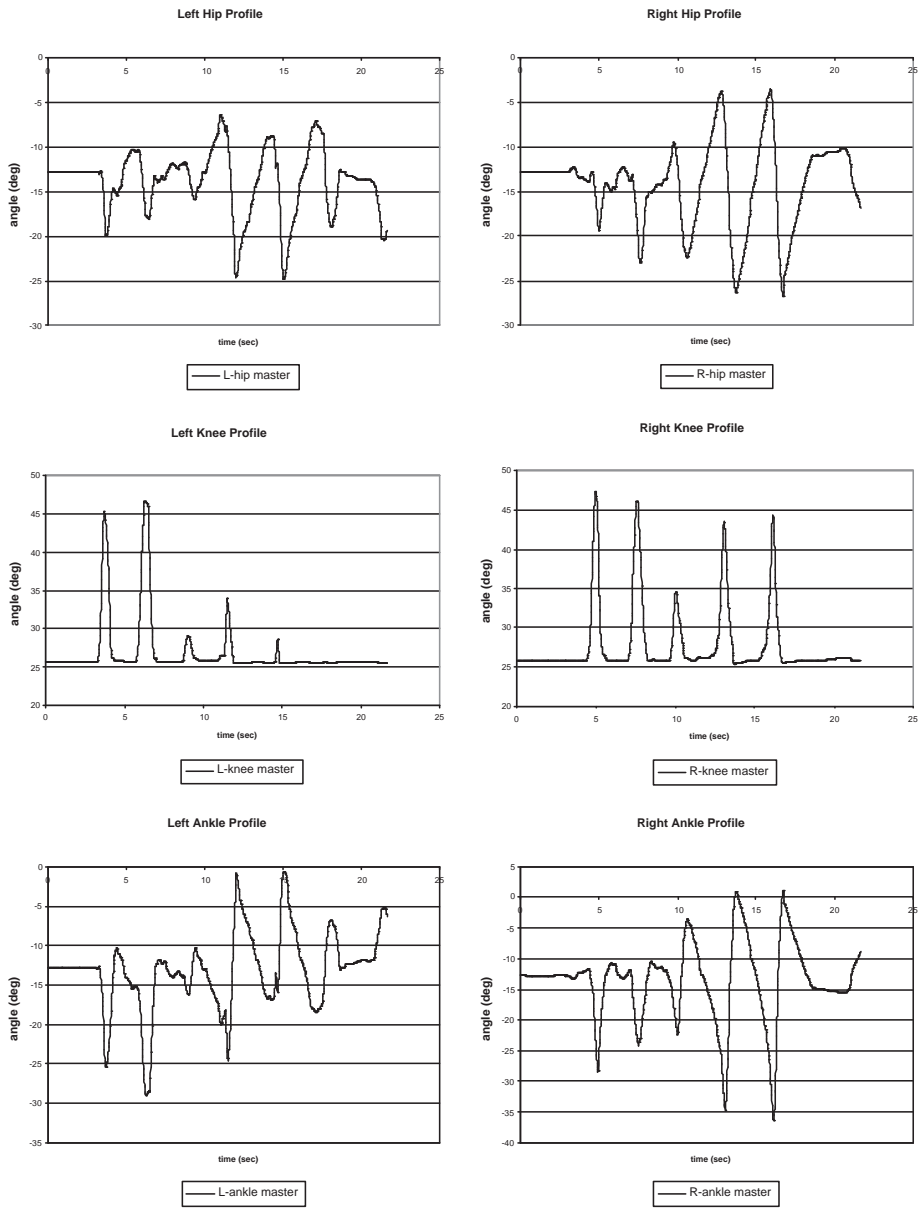


Figure 7.10: Leg joint trajectories for experiment 3.

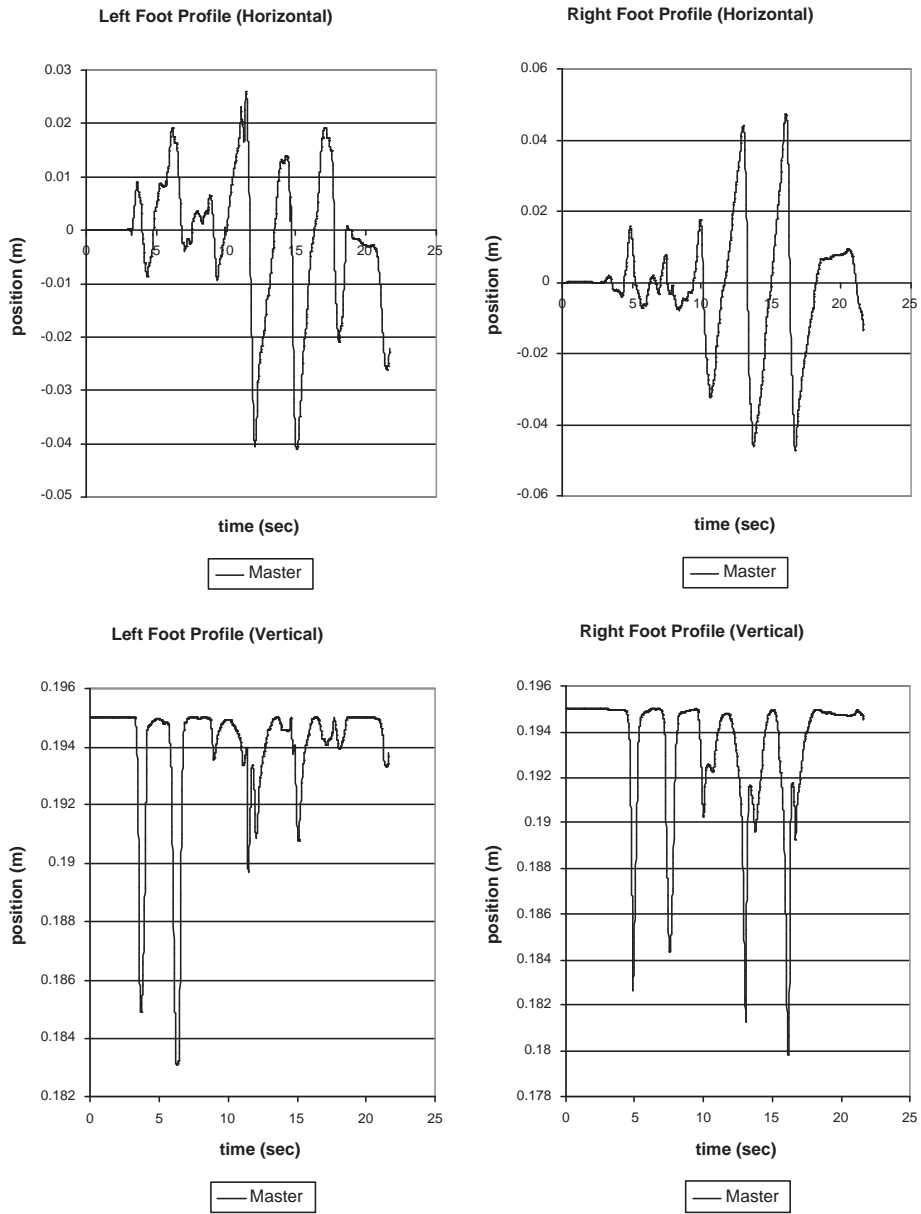


Figure 7.11: Foot trajectories for experiment 3.

7.4 Experiment 4 - Modification of Playback Time Interval

Experiment 4 is to test the the simulation result which claims that the slower walking speed of the humanoid robot will be more stable. The control method used is the mapping of foot position.

The procedure of the experiment is as follow:-

1. Foot position profile (x_{master} and y_{master}) is captured by master exoskeleton at a sampling rate of 15msec.
2. Foot position profile is being scaled to $\frac{1}{4}$ of the original. y_{master} is then modified to prevent singularities, in this case a decrease of 5mm has been used.
3. The corresponding joint profiles (ϑ_{hip} , ϑ_{knee} and ϑ_{ankle}) is then generated by inverse kinematics of the foot position profile (x_{slave} and y_{slave}).
4. The playback time interval is set to twice of the original , i.e. 30msec.

The experiment shows that even the humanoid robot walks in a slower manner, it does not exhibit any improvement in the stability. One of the major drawbacks of this kind of scaling, which is based on the increase of playback time interval, is the loss of coherence between the slave (humanoid robot) and the master (human operator). The loss of coherence basically means the walking behavior between the human operator and the humanoid robot is not in phase anymore. In addition to this delay of the motion, it is difficult for the human operator to control the robot - the human operator is expected to adapt a wait-and-see approach to achieve successful teleoperation. Not only this wait-and-see approach hinder the effectiveness and the performance of the teleoperation system, it will also increase the mental burden and physical fatigue of the human operator.

To ensure that the humanoid robot does not fall down during locomotion, the most common way is to ensure the ZMP is within the foothold at all time during the locomotion. In the case of teleoperation, the human operator needs to monitor the ZMP location and adjusts such that the overall stability of the humanoid is achieved. This process becomes impossible if such a time scaling method is used.

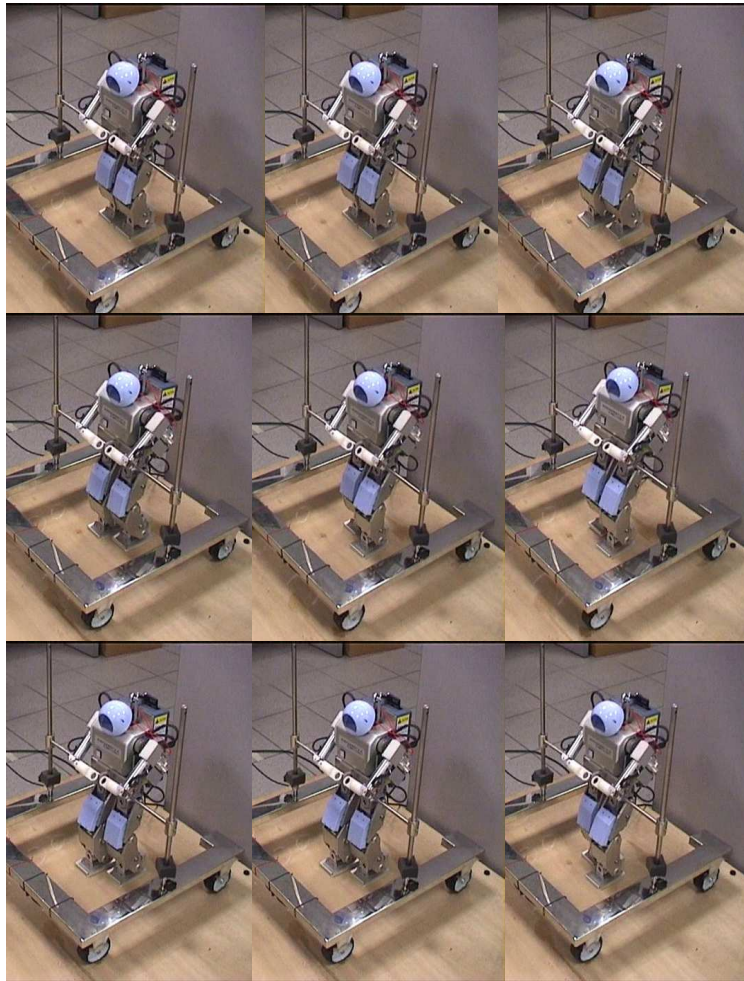


Figure 7.12: Snapshots of the experiment of scaling based on modification of playback time interval.

7.5 Experiment 5 - Modification of Walking Profile

Experiment 5 was carried out to investigate whether scaling down of the step length and step height will improve the walking stability of the humanoid robot. In this experiment the focus is on the modification of the joint profile of the robot such that the velocity profile of the slave robot is half of the master's.

The procedure of the experiment is as follows:-

1. Foot position profile (x_{master} and y_{master}) is captured by master exoskeleton at a sampling time interval of 15msec.
2. Generate a master velocity profile for each time interval.

$$\dot{x}_n = \frac{x_n - x_{n-1}}{\Delta t} \quad (7.1)$$

$$\dot{y}_n = \frac{y_n - y_{n-1}}{\Delta t} \quad (7.2)$$

for time step $n = 1, 2, 3, \dots$, and Δt is the sampling time interval.

3. Using the master velocity profile, slave velocity profile can be generated by using the relationship of $v_{slave} = \frac{1}{2}v_{master}$.
4. Foot position profile of slave can be generated.

$$x_n = x_{n-1} + \dot{x}_n \Delta t \quad (7.3)$$

$$y_n = y_{n-1} + \dot{y}_n \Delta t \quad (7.4)$$

for time step $n = 1, 2, 3, \dots$, and Δt is the sampling time interval.

5. The corresponding joint profiles (ϑ_{hip} , ϑ_{knee} and ϑ_{ankle}) are then generated by inverse kinematics of the foot position profile (x_{slave} and y_{slave}). The playback time interval is 15msec which is the same as the master.

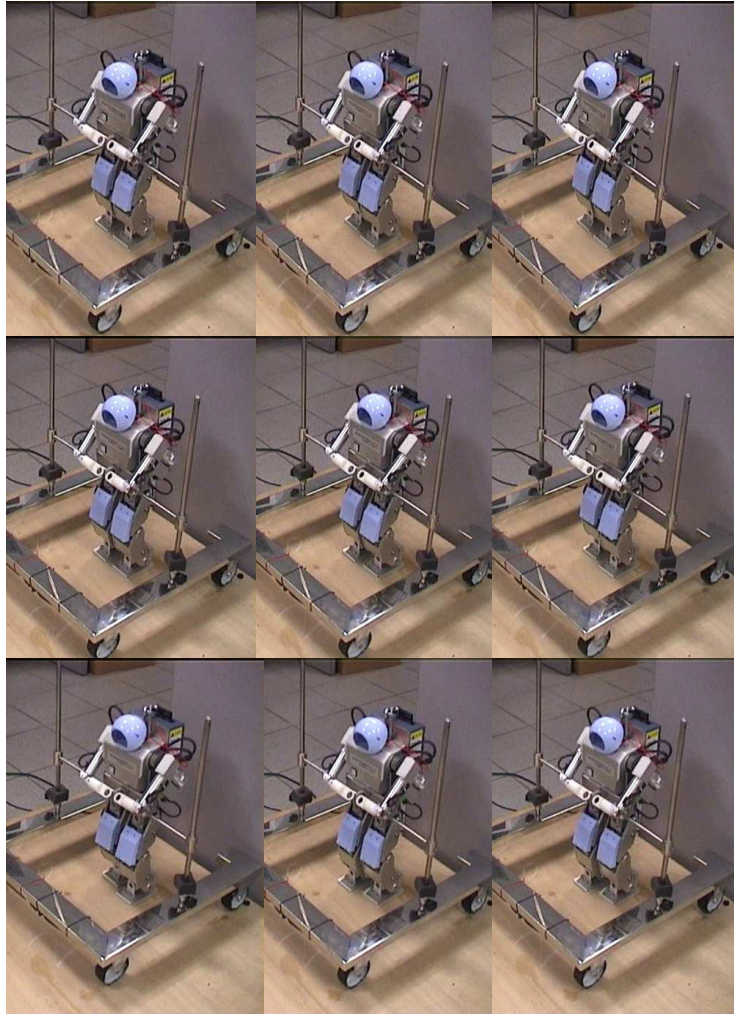


Figure 7.13: Snapshots of the experiment of scaling based on modification of walking profiles. Notice the small stride length and step height of the robot.

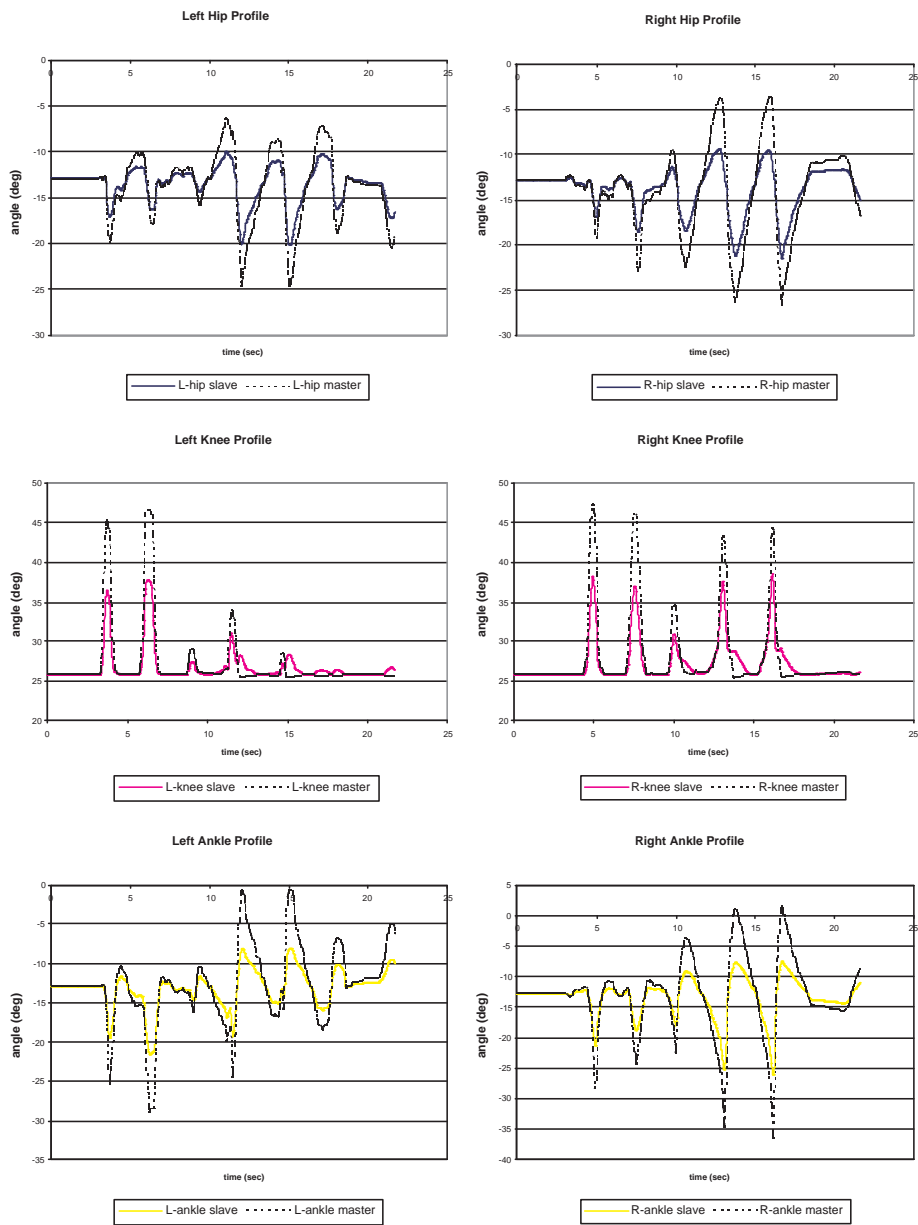


Figure 7.14: Leg joint trajectories for experiment 5. Blue: Hip; Magenta: Knee; Yellow: Ankle. Notice the scaling down of the joint angles of the slave compare with the master.

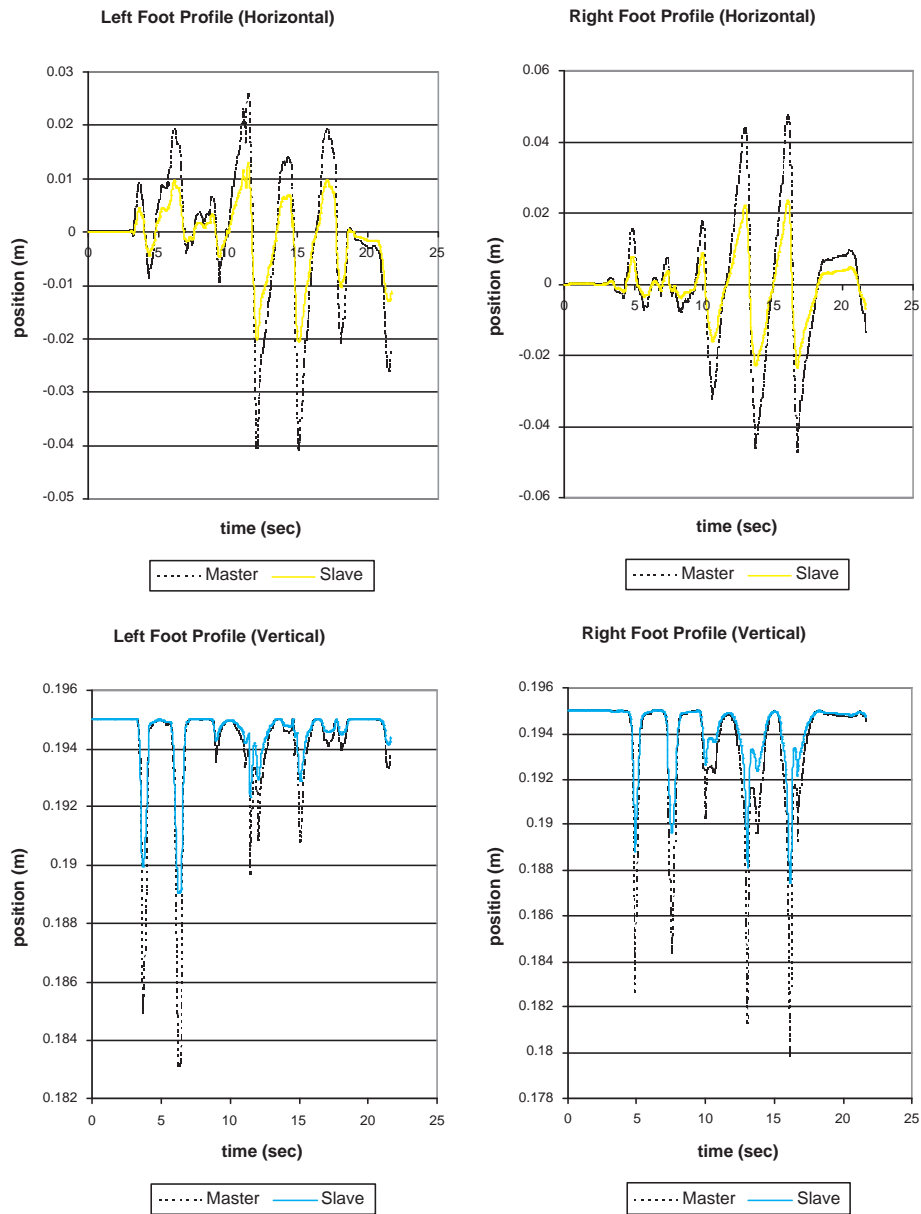


Figure 7.15: Foot trajectories for experiment 5. Blue: Vertical foot position; Yellow: Horizontal foot position. Notice the scaling down of the foot position of the slave compare with the master.

It is expected that this scaling method is better as the motion of the slave robot is teleoperated without any delay in motion. However, the experimental result shows otherwise. One of the major problem observed in this experiment is that due to the down-scaling of the velocity profile of the slave robot, the foot height clearance become smaller. The effect of this decrease in the clearance is magnified by the imperfection of the master exoskeleton and the position error of the humanoid robot. One way to solve this problem is to ask the human operator to perform exaggerate motion during teleoperation. However this is undesirable for obvious reason.

Chapter 8

Conclusion and Future Works

In this research project, a teleoperation system for humanoid is designed and constructed. This system is built to explore the possibility of a novel control method - teleoperation, on humanoid walking. The novelty of this control method is the application of a kinematic similar master exoskeleton which enable human operator to control the robot legs as if their own. This approach is expected to simplify and results in a more intuitive control of the humanoid, if compared with other teleoperation method such as supervisory control method adopted by (Hasunuma, 2002) and Hirai et al. (1998).

System architecture based on the master-PC-slave configuration has been developed. The master exoskeleton is the most critical part of the teleoperation system. The master exoskeleton consists of three major units - the waist unit, thigh unit and shank unit. The exclusion of the foot unit has been verified in the kinematic study section and the simulation section. Major dimensions of an average adult Chinese has been used in the design of the master exoskeleton. Personal computer is used as the interface and controller between the master and slave. The operating system used in the system is RT-Linux, for its real-time capabilities. Fujitsu humanoid robot (HOAP-1) is chosen to be the slave robot for its well-constructed mechanical structure and open source software. The smaller size of the slave robot also provide an opportunity of studying the necessary scaling between the master and slave.

Kinematic study and simulation has been conducted for the purpose of verification

of the feasibility of teleoperation. A comparison of the physical dimensions of human and Fujitsu humanoid robot ensure potential problem can be prevented. Regulation of foot such that humanoid robot is walking flat-footed with respect to the ground has been adopted in the simulation and experiment.

Simulation results gives an insight of the appropriate approach for teleoperation of small scaled robot. Interesting finding of a slight improvement on the stability on humanoid walking both on body pitch and ZMP based on Froude number scaling are presented in the latter part of simulation section. Despite a significant change in the duty factor of the gait, Froude number scaling still improve the performance of humanoid walking in simulation. Eventhough the improvement is slight in our case, we anticipate that dynamic similarity is possible to achieve if the human operator walks flat-footed, i.e. the duty factor of the gait is preserved.

To test the hardware and the control architecture of the teleoperation system, five different experiments have been carried out. Two different control methods - direct joint mapping and the mapping of foot position have been compared. The result shows the mapping of the foot position is a better method than the direct mapping of joints. It is somewhat expected as the imperfection of the master exoskeleton has more influence on the former method. The control method of mapping the foot position is less prone to the inaccurate tracking and errors of the master exoskeleton.

Experiments 4 and 5 conclude that the reduction of humanoid walking speed and scaled-down walking profile are both inappropriate. These two scaling not only fail to enhance the performance of the teleoperation, but also diminish the intuitive control by the human operator.

Improvement on Master Exoskeleton Improvement such as weight reduction and structural design can be implemented for future prototypes of the master exoskeleton. The first prototype of master exoskeleton is built for the purpose of anthropomorphism - the coincidence of the joints is the major consideration. With the weight (approximately 2kg) and the rigidity of the structure, it is quite uncomfortable for human operator to put on. A change of material with the properties of light weight and flexible, such as

plastic, should be considered. The 1st prototype also designed to fit average Chinese adult. Adjustable links should be included in the future design of the master exoskeleton.

Additional Camera Telepresence means the human operator can see and feel as if he is at the remote site. Stereo vision is crucial in the success of creating telepresence. With stereo vision, human operator can perceive objects and surroundings at remote site more precisely, especially those moving towards or away in the depth dimension. A camera needs to be incorporated with the slave robot such that visual feedback can be transmitted back to master site. The camera must have the capability of streaming at minimum 24fps, the threshold of smooth motion can be detected by human eye; lesser frame rate will cause dizziness.

References

- Alexander, R. McN. and Jayes, A. S. 1983. *A dynamic similarity hypothesis for the gaits of quadrupedal mammals*. J. Zool., Lond. 201, 135152.
- Chew, C.M. and Pratt, G.A., 2002. *Dynamic bipedal walking assisted by learning*. *Robotica* (20) pp. 447-491.
- Chew, C.M., Choong, E., Poo, A.N. and Hong, G.S., 2003. *From science fiction to reality - Humanoid robots*. HNICEM International conference March27-30, Manila, Philippines. pp. 1-10.
- Craig, J., 2002. *Introduction to robotics, mechnics and control* Pearson Education, Inc.
- Damon, A., 1966. *the human body in equipment design* Cambridge, Harvard U. P.
- FMSlabs, 2001. *Getting started with RT-Linux*. FMS Labs, Inc. 2001.
- Hannaford, B., 2000. *Feeling is believing: A history of telerobotics*. *The Robot in the Garden*. Eds. K. Goldberg, Cambridge, Massachusetts, The MIT Press, 246-276.
- Hasunuma, H., 2002. *A tele-operated humanoid robot drives a lift truck*. Proc. IEEE Intl. Conf. Robotics and Automation pp. 2246-2252.
- Hirai, 1985. *The development of honda humanoid robot*. Proc. IEEE Intl. Conf. Robotics and Automation pp. 1321-1326.
- Inman, V. T., Ralston, H. J., and Todd, F., 1994 *Human Locomotion*. Human Walking. Eds. Rose. J. and Gamble J. G., Baltimore, Williams & Wilkins, 1-27.
- Rose, J. and Gamble, J.G., 1993. *Human walking, second edition*. Williams & Wilkins, Baltimore, USA.
- Jalics, L., Hemami, H., and Zheng, Y.F., 1997. *Pattern generation using coupled oscillations for robotics and biorobotic adaptive periodic movement*. IEEE Intl. conf. on robotics and automation.
- Kajitha, S. and Tani, K., 1991. *Study of dynamic bipeda locomotion on rugged terrain*. IEEE Intl. conf. on robotics and automation pp. 1405-1411.
- Kajitha, S. and Tani, K., 1996. *Experimental study of biped dynamic walking*. IEEE Transactions on Control systems Feb, 1996 pp. 13-19.
- Kajitha, S., 2002. *Running pattern generation for a humnaoid robot*. IEEE Intl. conf. on robotics and automation pp. 2755-2761.

- Kaneko, T., 2002. *Design of advanced leg module for humanoid robotics project of METI*. Proc. IEEE Intl. Conf. Robotics and Automation pp. 38-45.
- Kenji, K., Kajata, S., Kanehiro, F., Yokoi, K., Fujiwara, K., 2002. *Design of advanced leg module for humanoid robotics project of METI*. Intl. conference on robotics & automation pp. 38-45.
- Kuroki, K., 2003. *A small biped entertainment robot exploring attractive applications*. Proc. IEEE Intl. Conf. Robotics and Automation pp. 471-476.
- Muybridge, E., 1955. *The human figure in motion*. New York: Dover Publications, Inc., 1955.
- Nordin, M. and Frankel, V. H. 2001. *Basic biomechanics of the musculoskeletal system*. Maryland: Lippincott Williams & Wilkins.
- Pratt, J., Chew, C.M., Torres, A., Dilworth, P. and Pratt, G., 2001. *Virtual model control: An intuitive approach for bipedal locomotion*. Intl. journal of robotics research (20:2) pp. 129-1433.
- Park, J.H. and Cho, H.C., 2000. *An online trajectory modifier for the base link of biped robots to enhanced locomotion stability*. Proc. IEEE Intl. Conf. Robotics and Automation pp. 3353-3358.
- Phesant, Nordin, M. and Frankel, V.H. 2001. *Bodyspace: anthropometry, ergonomics, and design..* London; Philadelphia: Taylor & Francis.
- Qiang, H., 2001. *Planning walking patterns for a biped robot*. IEEE transactions on robotics and automation Vol. 17(3). pp. 280-289.
- Sim, W.Y., Chew, C.M. and Hong, G.S., 2004. *The use of teleoperation for humanoid walking - A first look*. Proc. IEEE Conf. on Robotics, Automation and Mechatronics (RAM), Singapore.
- Taga, G., 1995. *A model of the neuro-musculo-skeletal system for human locomotion*. Biological Cybernetics, Vol 73, 97-111.
- Vertut, J., 1985. *Teleoperation and Robotics*. France: hermes Publising.
- Vukobratovic, M. and Jurij, S., 1973. *Mathematical models of general anthropomorphic systems*. Mathematical biosciences (17) pp. 191-242.
- Vukobratovic, M., Borovac, B., Surla, D. and Stokic, D., 1990. *Scientific fundamentals of robotics 7 - Bipedal locomotion*. Springer-Verlag, Berlin.
- Vukobratovic, M. and Borovac, B., 2004. *Zero moment point - thirty five years of its life*. International journal of humanoid robotics (1-1) pp. 157-173.
- Zielinska, T., 1996. *Coupled oscillators utilized as gait rhythm generators of a two legged walking machine*. Biological Cybernetics, Vol 74, 263-273.

WEBSITES

ASIMO, Honda. <http://world.honda.com/ASIMO/>

HRP-2P, Kawada industries. <http://www.kawada.co.jp/ams/hrp-2/index.e.html>

RTL mailing list, FMS labs. <http://www2.fsmlabs.com/mailman/listinfo/rtl>

QRIO, Sony. <http://www.sony.net/SonyInfo/QRIO/>

Wasida Humanoids robotics institute. <http://www.takanishi.mech.waseda.ac.jp/research/wabian/>

M2, Leg lab, MIT. <http://www.ai.mit.edu/projects/leglab/robots/robots.html>

Fujitsu Robot HOAP-1. <http://www.automation.fujitsu.com/products/products07.html>

Yobotics!. <http://yobotics.com>

Appendix A

Mass Property of Fujitsu Humanoid Robot

Table A1 shows the mechanical properties of the links of the Fujitsu humanoid robot used in simulation.

Table A.1: Mass Property of Fujitsu Humanoid Robot

BODY	<p>Mass 2.3355e+00 <i>kg</i></p> <p>Center of Gravity wrt RJ3-LINK-CS coordinate frame: (<i>kg * mm²</i>)</p> <p>X Y Z -2.770e+01 -2.08e-01 1.132e+02 mm</p> <p>I_{xx} I_{yy} I_{zz} 9.081e+03 8.9580e+03 5.138e+03</p>
R-Hip (RLEG-JOINT[3])	<p>Mass 4.635e-01 <i>kg</i></p> <p>Center of Gravity wrt RJ3-LINK-CS coordinate frame: (<i>kg * mm²</i>)</p> <p>X Y Z -2.525e+00 5.163e-01 3.594e+00 mm</p> <p>I_{xx} I_{yy} I_{zz} 2.286e+02 4.880e+02 4.120e+02</p>
R-knee (RLEG-JOINT[4])	<p>Mass = 2.860e-01 <i>kg</i></p> <p>Center of Gravity wrt RJ4-LINK-CS coordinate frame: (<i>kg * mm²</i>)</p> <p>X Y Z -4.265e+01 1.063e+01 4.310e-01 mm</p> <p>I_{xx} I_{yy} I_{zz} 1.816e+02 2.810e+02 1.846e+02</p>
R-ankle (RLEG-JOINT[5])	<p>Mass = 1.8502725e-01 <i>kg</i></p> <p>Center of Gravity wrt RJ5-LINK-CS coordinate frame: (<i>kg * mm²</i>)</p> <p>X Y Z 2.911e+00 3.442e+00 -6.445e-01 mm</p> <p>I_{xx} I_{yy} I_{zz} 6.240e+01 4.769e+01 5.423e+01</p>
L-Hip (LLEG-JOINT[3])	<p>Mass 4.684e-01 <i>kg</i></p> <p>Center of Gravity wrt LJ3-LINK-CS coordinate frame: (<i>kg * mm²</i>)</p> <p>X Y Z -7.496e+01 4.715e+00 1.020e+00 mm</p> <p>I_{xx} I_{yy} I_{zz} 2.332e+00 4.963e+02 4.192e+02</p>
L-knee (LLEG-JOINT[4])	<p>Mass = 2.8824333e-01 <i>kg</i></p> <p>Center of Gravity wrt LJ4-LINK-CS coordinate frame: (<i>kg * mm²</i>)</p> <p>X Y Z -4.272e+01 1.0716e+01 -4.177e-01 mm</p> <p>I_{xx} I_{yy} I_{zz} 1.841e+02 2.847e+02 1.874e+02</p>
L-ankle (LLEG-JOINT[5])	<p>Mass = 1.8111717e-01 <i>kg</i></p> <p>Center of Gravity wrt LJ5-LINK-CS coordinate frame: (<i>kg * mm²</i>)</p> <p>X Y Z 2.885e+00 3.505e+00 5.948e-01 mm</p> <p>I_{xx} I_{yy} I_{zz} 6.027e+01 4.547e+01 5.347e+01</p>